Cross-term Suppression in Wigner Distribution

by

Nabeel Ali Khan
PE083007

A thesis submitted to the
Electronic Engineering Department
in partial fulfillment of the requirements for the degree of
DOCTOR OF PHILOSOPHY IN ELECTRONIC ENGINEERING

Faculty of Engineering and Applied Sciences
Mohammad Ali Jinnah University
Islamabad

December 2010

Dedicated to my parents and wife

ACKNOWLEDGMENT

I would like to thank Dr. Imtiaz (my supervisor) and Dr. Noman Jafri(my co-supervisor) for their kind support and guidance.

ABSTRACT

Wigner Distribution, one of many methods to compute time frequency representation, satisfies large number of mathematical properties and gives optimal energy concentration in time frequency plane. However, Wigner distribution suffers from severe cross-term interference problem, which limits its scope for practical applications.

Different modified versions of Wigner distribution have been developed to overcome its cross-term interference problem. Most of these techniques suppresses cross-term on the expense of quality of auto-terms. Schemes that compleltely remove cross-terms without affecting the resolution of Wigner distribution are computationally very expensive.

This research proposes a computationally efficient solution to cross-term interference problem based on image processing and fractional filtering. Signal components are located in time frequency plane using image processing. Fractional filters are then applied to separate signal components. Wigner distribution of separated signal components is computed and added up to obtain cross-term free crisp time frequency representation. Performance of the proposed time frequency representation is evaluated both on synthetic and real life bat signals.

One of the most significant application of Wigner distribution is instantaneous frequency estimation of signals. However, Wigner distribution based instantaneous frequency can only be applied to mono-component signal because of its cross-term problem. In this study we extend Wigner distribution based instantaneous frequency estimation scheme to multi-component signals having non-overlapping time frequency representation.

LIST OF PUBLICATIONS

1) Nabeel Ali Khan, Imtiaz A Taj, M. Noman Jari, Salman Ijaz, 2011. Cross-term elimination in Wigner distribution based on 2D signal processing techniques. Signal Processing 91(3), 590-599, advances in Fractional Signals and Systems.

2) Nabeel Ali Khan, M. Noman Jaffri, Syed Ismail Shah, "Modified Gabor Wigner Transform for Crisp Time Frequency Representation," ICSAP, pp.119-122, 2009 International Conference on Signal Acquisition and Processing, 2009.

3) Nabeel Ali Khan, Imtiaz A. Taj, M. Noman Jaffri, "Instantaneous Frequency Estimation Using Fractional Fourier Transform and Wigner Distribution," ICSAP, pp.319-321, 2010 International Conference on Signal Acquisition and Processing, 2010

TABLE OF CONTENTS

LIST OF FIGURES

LIST OF TABLES

LIST OF ACRONYMS

Wigner Distribution	WD
Pseudo Wigner Distribution	PWD
Time-Frequency	t-f
Support Vector Machine	SVM
Fractional Fourier Transform	FrFT
Instantaneous Frequency	IF
Gabor Transform	GT
Gabor Wigner Transform	GWT
Cross-terms	CT
Zhao-Atlas-Marks	ZAM
Partial Differential Equation	PDE
Signal to Noise ratio	SNR
Intersection of the confidence interval	ICI

Chapter 1

INTRODUCTION

1.1 Background

Most of the real life signals are non-stationary as their spectral properties change with time. Such signals cannot be analyzed well by conventional signal analysis tools such as pure time domain and frequency domain representations. Both time and frequency domain representations separately do not give any information about time localization of frequencies.

Fortunately, joint time-frequency(t-f) representations have emerged as a powerful tool for the analysis of such signals. Joint t-f representation can be interpreted as a spread of signal energy in joint t-f plane. T-f representation gives information regarding signals which is otherwise hidden from analyst; such as number of signal components, their relative amplitude, their instantaneous frequencies and instantaneous bandwidths.

Several t-f representations have been proposed to date. These distributions can be broadly categorized into linear and quadratic distributions. T-f representations are often compared in terms of their resolution performance, mathematical properties and ability to suppress cross-terms(CT).

1.2 Objective

Wigner distribution (WD) satisfies large number of desirable mathematical properties, such as time and frequency marginal and shifts as discussed by Boashash (2003). It has a very high resolution and gives ideal estimate of IF for mono-component linear frequency modulated signals. WD with data driven window length can also be used for IF estimation of non-linearly frequency modulated signals as proposed by Katkovnik and Stankovic (1998). However, presence of

undesirable CT for multi-component and/or non-linearly modulated signals limits its practical significance as discussed by Boashash (2003). Many techniques have been proposed to suppress or completely remove CT of WD. Most of these techniques are either computationally too costly or suppress CT at the expense of energy concentration of auto-terms. The objective of this research is to propose a time frequency distribution with following salient features:

1. It should be computationally efficient.
2. Eliminate the CT of WD.
3. Auto-terms should not get blurred as a result of CT suppression.
4. Algorithm should be fully automatic.

1.3 The Proposed Methodology

We propose a novel scheme to suppress CT of WD for a multi-component signal. CT in WD can be categorized into two main catigories i.e outer-interference and inner-interference. Outer-interference arising due to multi-component nature of a signal can be eliminated by separating signal components by using some kind of time varying filter and computing WD of separated signal components. These separated signal components would still suffer from inner-interference terms that arise due to non-linear frequency modulation. Therefore, post processing of WD is necessary to suppress inner-interference terms. In this study we propose a combination of Gabor Wigner transform(GWT) proposed by Pei and Ding (2007) and fractional filtering to reduce CT.

In order to separate signal components we need to first locate them in t-f plane and then apply a time varying filter to separate them. Image processing technique of connected component segmentation is employed to locate signal components

in a t-f plane. Fractional Fourier transform (FrFT) is then employed as a time varying filter for separating signal components.

WD of separated signal components is computed to obtain t-f distributions which are free of outer-interference. However, these distribution would still suffer from inner-interference terms. These inner-interference terms are suppressed by computing GWT, defined as product of WD with short time Fourier transform, of separated signal components. Finally, GWTs of separated signal component are added up to obtain a t-f distribution with significantly reduced CT.

1.4 Contribution

Main contributions in this thesis are as follows

1. Mathematical Analysis of Gabor Wigner transform proposed by Pei and Ding (2007), one of many techniques to suppress CT of WD, and its limitations.
2. Hybrid image processing and fractional Fourier Transform based technique to compute almost interference free WD for multi-component signal.
3. IF estimation of a multi-component signal.

1.5 Thesis Organization

This thesis is organized into seven chapters whose contents are described below.

Chapter 1 presents the problem statement and contributions in this thesis. Organization of rest of thesis is also described in it. **Chapter 2** covers literature review. It starts with the review of Fourier transform and emphasizes the need for t-f analysis. Some of the state of the art techniques to compute t-f representations like Short time Fourier transform, Wavelet transform, WD, distributions from Cohen class, reassigned Cohen's distribution and some of the latest time frequency techniques are discussed and compared. **Chapter 3** presents the mathematical

analysis of GWT transform and discusses its limitations. **Chapter 4** describes proposed interference suppression technique. The proposed technique utilizes image processing to locate signal components and fractional filtering is employed for signal separation. WD of separated signal components is then computed and added up to obtain almost CT free t-f representation. **Chapter 5** compares the performance of proposed technique with other similar techniques. The performance of the proposed technique is evaluated in terms of energy concentration, CT suppression and computational cost. **Chapter 6** presents an interesting application of proposed t-f representation. The proposed technique for computing suppressed interference crisp t-f representation is applied for computation of instantaneous frequencies of a multi-component signal. The proposed technique extends the classical WD based mono-component IF estimator discussed by Katkovnik and Stankovic (1998) for multi-component signals. **Chapter 7** summarizes the main conclusions of thesis. It also provides directions for future work and improvements

Chapter 2

LITERATURE REVIEW

In this Chapter, a review of some of the most popular t-f signal analysis techniques is presented. Chapter starts with the brief discussion of Fourier transform and its limitations in dealing with non-stationary signals. This follows a discussion on linear and quadratic t-f representations. Two prominent distributions from linear class (i.e short time Fourier transform and wavelet transform) and two prominent distributions from quadratic class (i.e WD and spectrogram) are discussed. Given the excellent resolution performance of WD, last section of this chapter is dedicated to interference suppression techniques in WD.

2.1 Classical Signal Analysis Technique and need for t-f analysis

Both time and frequency domain representations of signal conveys useful information about its nature. Fourier transform relates time and frequency domain by following equation.

$$X(\omega) = \int x(t)e^{-j\omega t} \qquad \textit{Eq (2.1)}$$

$X(\omega)$ and $x(t)$ are time and frequency domain representations of a signal respectively. Objective of using Fourier analysis is to break the signal into stationary frequency components and compute their relative amplitudes. $X(\omega)$ is a complex quantity, therefore it can be represented by magnitude and phase spectra. For many signals, frequency domain representation is more informative.

In the definition of the Fourier transform, the stationary nature of the signal is assumed, i.e. the spectrum is assumed to be independent of time and all signal frequency components are assumed to exist for the entire time duration of the signal. The magnitude spectrum only gives information regarding number of frequency

components present in the signal and their respective amplitudes. It does not tell anything about the frequency modulation laws of the components and their time duration. Unless the components are disjoint in frequency for the entire duration of the signal, the spectrum also gives no information about the frequency bands signal components occupy.

Most of the real signals are non-stationary and vary with time. Such signals have time varying spectra and cannot be analyzed separately in time and frequency domains. Such signals are best analyzed jointly using t-f representations. Joint t-f analysis gives the information that cannot be obtained in either time or frequency domains, such as; various signal components, their relative amplitudes, time and frequency bands in which they are defined. T-f analysis also provides time localization of frequencies.

In order to emphasize the need for t-f analysis, a time varying signal composed of two linear chirps is being considered. Both time domain representation shown in Fig 2.1(a) and frequency domain representation shown in Fig 2.1(b) fail to classify signal as multi-component or mono-component. Whereas, joint t-f representation shown in Fig 2.1(c) clearly shows that signal is composed of two components. Moreover, information regarding starting and ending time of respective signal components and their frequency modulation laws can also be obtained from the given t-f representation.

2.2 Time Frequency Techniques

This section introduces some of the basic t-f signal analysis tools like IF, short time Fourier transform, WD and Wavelet transform.

2.2.1 Instantaneous Frequency

One way to obtain time localization of frequencies in a signal is to compute its IF, where IF of signal is defined as derivative of the phase of a signal. Mathematically,

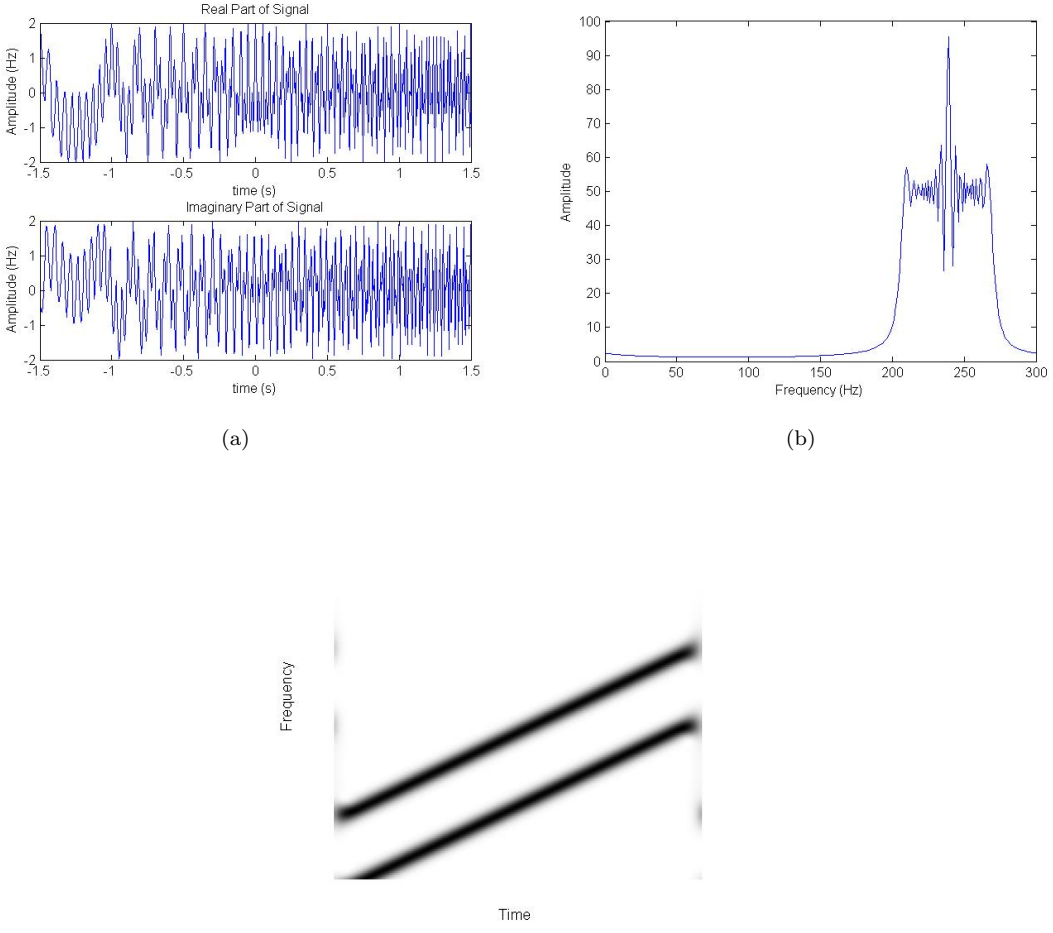

(a) (b)

(c)

FIGURE 2.1: (a) Signal in time domain (b) Signal in Frequency domain (c) Signal in joint t-f domain

$$\omega(t) = \frac{1}{2\pi}\frac{d}{dt}arg(x(t)), \qquad Eq\ (2.2)$$

where $x(t)$ is analytic signal of real signal $s(t)$. Mathematically,

$$x(t) = s(t) + js(t) * \frac{1}{\pi t}. \qquad Eq\ (2.3)$$

It gives perfect time localization of frequency. However, time localization of frequencies, by computing derivative of phase, can only be obtained for mono-component signals. Review of IF estimation techniques can be found in section

6.1.

2.2.2 Linear Time frequency representations

All those t-f representations that obey principle of superposition can be classified as linear distributions as discussed by Hlawatsch and Boudreaux-Bartels (1992). Mathematically,

$$s(t) = s_1(t) + s_2(t) \qquad Eq\ (2.4)$$

$$TF_{s(t)}(t,\omega) = TF_{s_1(t)}(t,\omega) + TF_{s_2(t)}(t,\omega) \qquad Eq\ (2.5)$$

Two popular linear t-f distributions i.e Wavelets and Short Time Fourier transform are discussed in following two subsections.

2.2.2.1 Short time Fourier Transform

Short time Fourier transform, as given by Cohen (1989), is defined as

$$STFT_{s(t)}(t,\omega) = \int h(\tau)s(\tau - t)e^{-j\omega\tau}d\tau \qquad Eq\ (2.6)$$

Signal is windowed in time by multiplying $h(\tau)$ window with $s(\tau - t)$. The Fourier transform of the local signal gives the local spectrum at specified time t. Short time Fourier transform is highly dependent on the shape and size of window. Long windows gives good frequency resolution and poor time resolution while short windows gives good time resolution, but poor frequency resolution.

2.2.2.2 Wavelet Transform

Continuous Wavelet transform as discussed by Lang (1999) can be considered an extension of Short time Fourier transform in which length of window is made a frequency dependent parameter. Mathematically,

$$WT(t,\omega) = \int s(\tau)w((\tau - t)\omega)\omega d\tau, \qquad Eq\ (2.7)$$

where $w(t)$ combines the complex exponential and Gaussian. Mathematically,

$$w(t) = \frac{1}{h\sqrt{2\pi}} e^{jt} e^{\frac{-t^2}{2h^2}} \qquad Eq\ (2.8)$$

Higher frequencies are better resolved in both time and frequency by smaller windows while lower frequencies are better resolved in frequency by larger window. Wavelet transform thus caters this need and width of window is varied accordingly. Though wavelet may improve resolution of short Time Fourier Transform, but it also suffers from same resolution limit as that of Short Time Fourier transform.

2.2.3 Quadratic Time Frequency Distributions

Linearity is a desired criterion for t-f representations. However, t-f representations can be interpreted as energy distributions. Therefore, t-f representations are expected to fulfill the following marginal criteria. Mathematically,

$$\int TF_s(t,\omega)d\omega = s^2(t) \qquad Eq\ (2.9)$$

$$\int TF_s(t,\omega)dt = s^2(\omega) \qquad Eq\ (2.10)$$

In addition from marginal criteria, quadratic t-f representations offer better resolution and are expected to fulfill large number of other mathematical properties. Spectrogram and WD are the two most popular quadratic t-f representations.

2.2.3.1 Spectrogram

Spectrogram is defined as squared modulus of short time Fourier transform. Mathematically,

$$SPEC_s(t,\omega) = STFT_s(t,\omega)STFT_s^*(t,\omega) \qquad Eq\ (2.11)$$

Spectrogram reduces in to linear transformation provided that short time Fourier transform of different components does not overlap in t-f plane. However, Spectrogram suffers from same window related resolution limitations as that of short time Fourier transform. Therefore, it gives blurred t-f representation. Different variants of Spectrogram have been developed to improve its resolution in time and frequency. These include Reassigned spectrogram by Fulop and Fitz (2006); Auger and Flandrin (1995), de-blurring of spectrogram using neural networks by Shafi et al. (2007), de-blurring using Image de-convolution techniques by kai Lu and Zhang (2009), optimal window selection by Baraniuk and Jones (1993), and Spectrogram using windows in fractional domain by Capus and Brown (2003). All of these techniques are either too slow or they cannot completely remove the blurring.

2.2.3.2 Wigner Distribution

WD is defined as Fourier transform of instantaneous auto-correlation function. Mathematically,

$$WD_s(t,\omega) = \int s(t-\frac{\tau}{2})s^*(t+\frac{\tau}{2})e^{-j\omega\tau}d\tau \qquad Eq\ (2.12)$$

WD fulfills large number of mathematical properties discussed by Boashash (2003), such as

1. Reality: WD is real for all values of t and ω.
2. Time Invariance: If signal is shifted in time domain its WD will also get shifted by the same amount along time axis. Mathematically,

$$s_\lambda(t) = s(t-t_0) \qquad Eq\ (2.13)$$

$$WD_{s_\lambda}(t,\omega) = WD_s(t-t_0,\omega) \qquad Eq\ (2.14)$$

3. Frequency Shift Invariance: If a signal is modulated(shifted) in frequency domain, then the same shift will occur in frequency axis of its WD

$$s_m(t) = s(t)e^{j\omega_0 t} \qquad Eq\ (2.15)$$

$$WD_{s_m}(t,\omega) = WD_s(t,\omega-\omega_0) \qquad Eq\ (2.16)$$

4. Time Marginal: Integration of WD along frequency axis gives signal energy distribution. Mathematically,

$$|s(t)|^2 = \int WD(t,\omega)d\omega \qquad Eq\ (2.17)$$

5. Frequency Marginal: Integration of WD along time axis gives energy spectrum.

$$|s(\omega)|^2 = \int WD(t,\omega)dt \qquad Eq\ (2.18)$$

6. Signal Energy: Integration of WD along both axis gives the signal energy.

7. Instantaneous Frequency: First order moment of WD along frequency axis gives instantaneous frequency.

$$\frac{\int \omega WD(t,\omega)d\omega}{\int WD(t,\omega)d\omega} = \frac{d}{d\omega}(args(t)) \qquad Eq\ (2.19)$$

8. Group Delay: Group delay can be computed from WD by computing its first moment with respect to time

$$\frac{\int tWD(t,\omega)dt}{\int WD(t,\omega)dt} = \frac{d}{dt}(args(\omega)) \qquad Eq\ (2.20)$$

9. Time Support: If signal does not exist outside interval $[t_1, t_2]$ then its WD will also not exist beyond this interval.

10. Frequency Support: If signal does not exist outside interval $[\omega_1, \omega_2]$ then its WD will also not exist beyond this interval.

11. Convolution Invariance: If two signals get convolved in time domain then their WD would also get convolved along time axis. Mathematically,

$$s(t) = s_1(t) * s_2(t) \qquad Eq\ (2.21)$$

$$WD_s(t,\omega) = WD_{s_1}(t,\omega) *_t WD_{s_2}(t,\omega) \qquad Eq\ (2.22)$$

12. Modulation Invariance: Multiplication of two signals in time domain results in convolution of respective WD along frequency axis. Mathematically,

$$s(t) = s_1(t) s_2(t) \qquad Eq\ (2.23)$$

$$WD_s(t,\omega) = WD_{s_1}(t,\omega) *_\omega WD_{s_2}(t,\omega) \qquad Eq\ (2.24)$$

13. Inner Product Invariance: The WD is a unitary transformation, therefore it preserves the inner product. Mathematically,

$$\int\int WD_{s_1}(t,\omega) WD_{s_2}(t,\omega) dt d\omega = \left| \int s_1(t) s_2^*(t) dt \right|^2 \qquad Eq\ (2.25)$$

In addition to these excellent mathematical properties, WD provides ideal energy concentration (delta function along IF)for linearly frequency modulated signals as demonstrated by Boashash (2003).

2.2.3.3 Limitations of WD

Major limitation of WD is the presence of undesired CT which have no physical meaning. CT can be categorized in two broad categories:

- Inner interference terms: These terms arise for non-linearly frequency modulated signals and can be understood by considering the example of parabolic chirp signal shown in Fig 2.2. Peak of its WD is highly concentrated along its IF. However, its energy concentration is poorer.

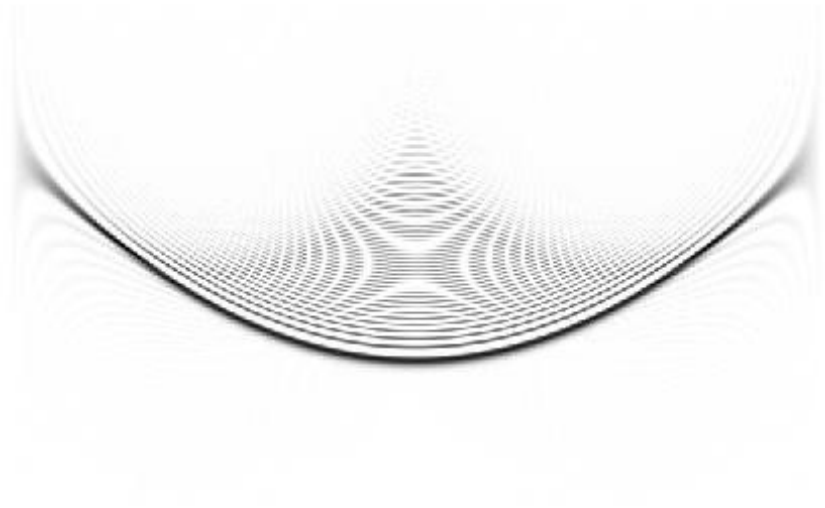

FIGURE 2.2: WD of parabolic chirp suffering from inner interference

- Outer interference terms: WD is quadratic in nature therefore CT also appear for signals composed of more than one component. Interference terms can be better understood by considering an example of signal composed of two components $s(t) = s_1(t) + s_2(t)$. WD of signal would be

$$WD_s(t,\omega) = WD_{s_1}(t,\omega) + WD_{s_2}(t,\omega) + 2Real\{\int s_1(t+\frac{\tau}{2}) s_2^*(t-\frac{\tau}{2}) e^{-j\omega\tau} d\tau\} \quad \textit{Eq (2.26)}$$

The last term in above expression represents a CT. CT are oscillatory in nature and are located midway between two components. The direction of isolation is normal to straight line connecting two components. For N component signal there would be $N(N-1)/2$ CT. CT appearing for multi-component signal can be demonstrated by considering an example of multi-component signal, whose spectrogram is given in Fig 2.3(a) and WD in Fig 2.3(b). It is clear from these figures that Spectrogram shows two chirps while WD shows three chirps. Third chirp appeared due to CT.

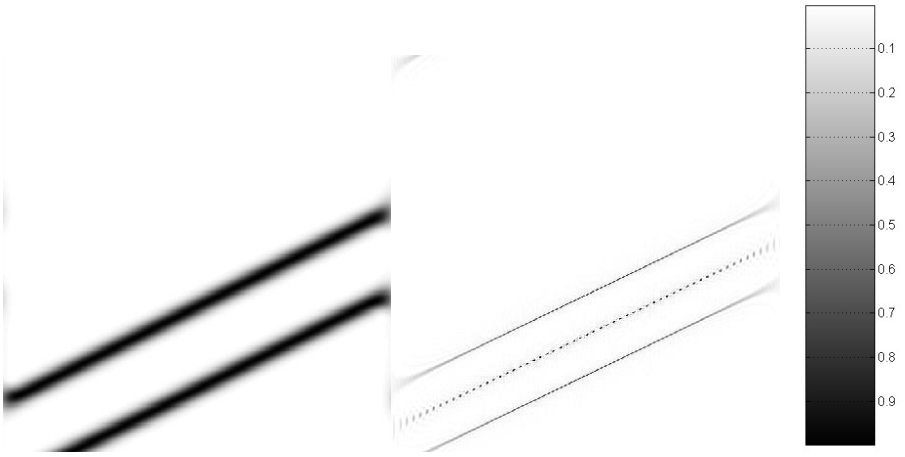

(a) (b)

FIGURE 2.3: (a)GT (b) WD

Presence of CT severely limits practical applications of WD. Various modified version of WD have been developed to overcome the problem of CT. These technique include distributions from Cohen's class Cohen (1989), Non-linear filtering of WD by Arce and Hasan (2000), S-Method by Stankovic (1994), Polynomial WD by Boashash and O'Shea (1994), GWT by Pei and Ding (2007), interference suppression using FrFT by Qazi et al. (2007).

2.3 Cross-term suppression techniques for WD

Given the mathematical properties of WD and its ability to give optimum energy concentration in t-f plane, many techniques have been proposed to overcome its limitation while dealing with multi-components signals or signals with non-linear frequency modulation laws. This section reviews existing interference suppression techniques. Objective of all these techniques are

1. To suppress/ eliminate CT
2. To preserve the quality of auto-terms
3. To be computationally efficient

However, for most of techniques there is a trade off between criteria (1) and criteria (2).

2.3.1 Cohen's Distributions

Cohen (1989) showed that all distributions from this class i.e. Choi-Williams, Gauss-Jordan, etc can be obtained from WD by convolving it with a 2D Kernel. Mathematically,

$$TF_s(t,\omega) = \int\int WD(t-t^{'},\omega-t^{'})\Psi(t^{'},\omega^{'})dt^{'}d\omega^{'} \qquad Eq\ (2.27)$$

Each member of Cohen's class differs in choice of Kernels. CT are generally suppressed as a result of convolution. However, auto-terms also get blurred. All distributions of Cohen's class generally satisfy time and frequency shifts that is, if $s(t)$ is delayed in time, and frequency modulated, then its t-f representation will be shifted by the same amount in both axes. Mathematically,

$$s_0(t) = s(t-t_0)e^{j\omega_0 t} \qquad Eq\ (2.28)$$

$$TF_{s_0} = TF_s(t-t_0,\omega-\omega_0) \qquad Eq\ (2.29)$$

CT suppression methods based on convolution of 2D kernel function with WD can be broadly classified into two categories

1. Fixed Kernel
2. Signal Dependent Kernels

2.3.1.1 Fixed Kernel

Fixed Kernel representations are obtained by convolving WD by a pre-determined kernel. Performance comparison of some of these kernels is given by Hlawatsch et al. (1995).

2.3.1.2 Signal dependent Kernel Representations

All kernel based t-f representations compromises CT suppression over auto-term quality. Hlawatsch et al. (1995) demonstrated that all fixed kernel based t-f representations are suitable for only a class of signals and are not general.

In order to overcome this limitation of fixed kernel t-f representation Baraniuk and Jones (1993) proposed an optimization method to compute a signal dependent kernel. Their proposed technique performs well for relatively large number of signals. However, major limitation of their scheme is that it computes one optimum kernel for whole signal and do not adapt kernel with respect to changing characteristics of signal.

Jones and Baraniuk (1995) proposed an adaptive signal dependent t-f representation which computes optimum kernel on block by block basis. Better results are obtained with this method at the expense of increased computational cost.

2.3.2 Reassigned Time frequency distributions

Smoothing of WD by signal dependent/ independent kernel reduces CT at the expense of quality of auto-terms. Reassignment method partially overcome this problem by shifting back the auto-terms. Closely looking at 2.27 reveals that t-f representation at any point (t, ω) is weighted sum of all neighboring points in t-f plane. This averaging may suppress CT, but also disturb the location of auto-terms. Reassignment method works on the principle that every point in t-f representation is shifted back to the center of gravity of the local neighborhood of t-f distribution. Co-efficients are calculated by following equation

$$t^{'}(t,\omega) = t - \frac{\int\int t_0 \psi(t_0,\omega_0) WD_s(t-t_0,\omega-\omega_0) dt_0 d\omega_0}{\int\int \psi(t_0,\omega_0) WD_s(t-t_0,\omega-\omega_0) dt_0 d\omega_0} \qquad Eq\ (2.30)$$

$$\omega^{'}(t,\omega) = \omega - \frac{\int\int \omega_0 \psi(t_0,\omega_0) WD_s(t-t_0,\omega-\omega_0) dt_0 d\omega_0}{\int\int \psi(t_0,\omega_0) WD_s(t-t_0,\omega-\omega_0) dt_0 d\omega_0} \qquad Eq\ (2.31)$$

A modified t-f representation given as result of reassignment is given as

$$MTF_s(t,\omega) = \int\int TF_s(t_0,\omega_0)\delta(t - t^{'}(t_0,\omega_0))\delta(\omega - \omega^{'}(t_0,\omega_0))d\omega_0 dt_0 \quad Eq\ (2.32)$$

The readability of resultant t-f representation is highly dependent on CT suppression and auto-term preservation capability of original t-f representation. Moreover, some desired mathematical properties of modified t-f representation may be lost for the sake of improved resolution.

2.3.3 Non-linear Filtering

All signal dependent/ independent methods suffer from trade off between auto-terms quality vs. CT suppression. Arce and Hasan (2000) proposed a non-linear filtering technique to suppress the CT of WD without much affecting auto term quality.

Their filter is based on intuition that auto-terms dominant regions have significantly less variation as compared to CT dominant regions. Thus in regions of low variation their proposed filter converts itself into close to identity operator while in regions of CT it becomes a low pass filter. Non-linear filtering technique performs significantly better than kernel based techniques but regions where auto-terms overlap CT their technique fail to give optimum results.

2.3.4 S-Method

In order to maintain auto-term quality, as high as in WD, while reducing CT, S-Method was proposed by Stankovic (1994).

$$SM(t,\omega) = \int P(\theta)STFT^{*}(t,\omega+\theta)STFT(t,\omega-\theta)d\theta \quad Eq\ (2.33)$$

$STFT(t,\omega)$ is short time Fourier transform. $P(\theta)$ controls the CT reduction. For $P(\theta) = \delta(\theta)$ above transformation becomes a Spectrogram and for $P(\theta) = 1$ it

becomes a WD. By carefully choosing length of $P(\theta)$, CT free t-f representation with auto-term quality close to WD can be obtained. However, this requires signal components to be distantly placed in t-f domain.

2.3.5 Adaptive S-Method

Major limitation of S-method was selecting the size of window. Shorter window would result in lesser resolution while longer windows may cause CT. This problem was solved by Stankovic and Stankovic (1997). They proposed a scheme for automatic window length selection. Thus, for t-f separable signals, a t-f representation that is free of CT and has auto-term quality equal to that of WD is achieved with the application of this method.

2.3.6 Polynomial Wigner Distribution

WD gives ideal t-f concentration for linear frequency modulated signals, however, for non-linearly frequency modulated signals WD suffers from CT. Boashash and O'Shea (1994) proposed Polynomial WD that extends WD for the class of signals which have instantaneous frequency variations of higher order. Mathematically,

$$WD_s(t,\omega) = \int s^2(t+\frac{\tau}{4})s^{*2}(t-\frac{\tau}{4})s(t+A\frac{\tau}{2})s^*(t+A\frac{\tau}{2})e^{\frac{-j\omega}{2.7}\tau}d\tau. \qquad Eq\ (2.34)$$

Polynomial WD has even more CT than simple WD for a multi-component signal. Thus this scheme is not general and limited to mono-component signals only.

2.3.7 Gabor Wigner Transform

Recently Pei and Ding (2007) proposed a GWT to combine the advantages of both Short time Fourier transform and Wigner transform. GWT is defined as product of GT and WD. Mathematically,

$$GWT_s(t,\omega) = WD_s(t,\omega)GT_s(t,\omega). \qquad Eq\ (2.35)$$

$GT_s(t,\omega)$ is a short time Fourier transform with Gaussian window. GWT eliminates CT of WD while maintaining clarity of auto-terms. However, it fails to give optimum results when CT of WD overlap auto-terms in t-f plane.

2.3.8 Cross-terms deleted Wigner Distribution using Bessel function expansion

Pachori and Sircar (2007) showed that by using Fourier Bessel expansion a multi-component signal can be decomposed into a number of mono-component signals. Mono-component signals are analyzed separately using WD and finally all WD are added to give a CT free representation. Major limitation of their technique is that it requires signal components to be separable in frequency domain and cannot be applied for signals whose components are separable in joint t-f domain but are not separable in just frequency domain. Moreover, their technique requires human intervention to locate signal components and is not automatic.

2.3.9 Matching Pursuit Algorithm

One way to compute CT free WD is to decompose a signal into a sum of of t-f atoms and compute WD of individual signal component. Matching Pursuit algorithm presented by Mallat and Zhang (1993) decomposes a signal into linear sum of t-f atoms chosen from redundant dictionary. Mathematically,

$$s(t) = \sum_{n=1}^{N} < s(t) g_{\lambda n} > g_{\lambda n} + R^m s(t). \qquad \textit{Eq (2.36)}$$

R^m is the residual vector. $g_{\lambda n}$ is time shifted and frequency modulated t-f atom given as

$$g_\lambda(t) = \frac{1}{\sqrt{s}} g(\frac{t-u}{s}) e^{j\xi t} \qquad \textit{Eq (2.37)}$$

and $\lambda = (s, u, \xi)$. WD of decomposed signals is computed and added up to give CT free t-f representation. Mathematically,

$$TF(t,\omega) = \sum_{n=1}^{N} < s(t) g_{\lambda n} > TF_{(g_{\lambda n})}(t,\omega) \qquad Eq\ (2.38)$$

Matching pursuit algorithm does not suffer from CT suppression and auto-term quality trade off. However, performance of this technique is highly dependent on choice of dictionary and prior knowledge of signals.

2.3.10 Fractional Fourier Based Interference suppression in Wigner Distribution

Recently some fractional Fourier based t-f techniques have emerged, that uses recently developed FrFT to compute signal dependent window. Traditionally choice of window depends upon the shape (Gaussian, Hamming, Hanning etc) and length. However, FrFT provides another degree of freedom i.e. rotation order.

2.3.10.1 S-Method in Fractional Fourier Domain

Capus and Brown (2003) demonstrated that resolution of short time Fourier transform can be increased by computing a signal dependent window in FrFT domain. Order of window in fractional Fourier domain is estimated from the second order variance of FrFT of signal. Their proposed scheme could resolve closely place chirps which ordinary Short time Fourier transform could not resolve.

Bastiaans et al. (2002) proposed a modification in S-Method to improve its resolution. Their proposed scheme utilized short time FrFT for convolution operation instead of ordinary short time Fourier transform. Experimental results demonstrated significant improvement in terms of CT elimination and auto-term preservation. However, finding an optimal fractional Fourier domain window is not possible for signals that are composed of multiple chirps with different frequency modulation laws.

2.3.10.2 Cross-term suppression using signal synthesis and fractional Fourier transform

Recently, Qazi et al. (2007) has proposed a fractional Fourier based recursive technique to eliminate CT without effecting auto-term quality. Moreover, their proposed technique performs well in highly challenging scenarios i.e. when auto-terms overlap CT.

Their technique exploits variance along various fractionally rotated and aligned back WDs to identify CT. CT are deleted by simply applying a mask containing zeros in areas of CT and ones in all other areas. Signal is synthesized from CT deleted WD by the signal synthesis technique given by Boudreaux-Bartels and Parks (1986). Synthesized signal is subtracted from original signal. If there were no CT overlapping auto-terms than subtracted signal would have zero energy and algorithm will stop. Other wise same procedure is recursively repeated for a subtracted signal. Finally, WDs composed of only auto-terms are added to give high quality t-f representation.

Only limitation of this scheme is its computational cost and iterative nature which limits its scope for parallel implementation.

Chapter 3

CRITICAL ANALYSIS OF GABOR WIGNER TRANSFORM

Recently Pei and Ding (2007) proposed a GWT to combine the advantages of both GT and WD. GT is free of CT while WD offers a higher resolution. Mathematically,

$$GWT(t,\omega) = WD(t,\omega)GT(t,\omega). \qquad Eq\ (3.1)$$

It will be shown that GWT offers considerable improvement in terms of CT reduction. However, in scenario of auto-terms overlapping CT, GWT would not give optimum results as demonstrated in our ealier work Khan et al. (2009).

3.1 Limitations of Gabor Wigner transform

In order to study the CT in GWT for a multi-component signal, we consider a signal composed of N number of components $s_i(t)$.

$$s(t) = \sum_{i=1}^{N} s_i(t). \qquad Eq\ (3.2)$$

WD of $s(t)$ is given by,

$$WD_s(t,\omega) = \sum_{i=1}^{N} WD_{s_i s_i}(t,\omega) + \sum_{\substack{j=1 \\ j\neq k}}^{N}\sum_{k=1}^{N} WD_{s_j s_k(t,\omega)}, \qquad Eq\ (3.3)$$

where,

$$WD_{s_{ii}}(t,\omega) = \int s_i(t-\frac{\tau}{2})s_i^*(t+\frac{\tau}{2})e^{-j\omega\tau}d\tau \qquad Eq\ (3.4)$$

$$WD_{s_{jk}}(t,\omega) = \int s_j(t-\frac{\tau}{2})s_k^*(t+\frac{\tau}{2})e^{-j\omega\tau}d\tau. \qquad Eq\ (3.5)$$

GT is just the Short time Fourier transform with Gaussian window function.

$$GT_s(t,\omega) = \int h(\tau - t)s(\tau)e^{-j\omega\tau}d\tau, \qquad \textit{Eq (3.6)}$$

where $h(\tau)$ is a Gaussian window. Short time Fourier Transform is a linear transformation and does not suffer from CT problem. However, it blurs t-f plane. Mathematically,

$$GT_s(t,\omega) = \sum_{i=1}^{N} GT_{s_i}(t,\omega), \qquad \textit{Eq (3.7)}$$

where $GT_{s_i}(t,\omega)$ is GT of signal component $s_i(t)$. GWT is defined as multiplication of WD and GT. Mathematically,

$$GWT(t,\omega) = WD(t,\omega)GT(t,\omega). \qquad \textit{Eq (3.8)}$$

It is assumed that two different signals have non-overlapping t-f signature, therefore the product of their t-f representations will be zero. This reduces above equation into

$$GWT_s(t,\omega) = \sum_{i=1}^{N} GT_{s_i}(t,\omega)WD_{s_i}(t,\omega) + \sum_{i=1}^{N}\sum_{\substack{j=1\\ j\neq k}}^{N}\sum_{k=1}^{N} GT_{s_i}(t,\omega)WD_{s_j s_k}(t,\omega). \qquad \textit{Eq (3.9)}$$

If CT of WD of a signal do not overlap with support region of GT that is

$$\sum_{i=1}^{N}\sum_{\substack{j=1\\ j\neq k}}^{N}\sum_{k=1}^{N} GT_{s_i}(t,\omega)WD_{s_j s_k}(t,\omega) = 0, \qquad \textit{Eq (3.10)}$$

then GWT becomes a linear transformation. Mathematically,

$$GWT_s(t,\omega) = \sum_{i=1}^{N} GWT_{s_i}(t,\omega). \qquad \textit{Eq (3.11)}$$

GT transform is CT free blurred image of WD distributions. Multiplying GT and WD results in an image, which is de-blurred and free of CT only if auto-terms do not overlap CT.

3.2 Experimental Results

We consider three examples to demonstrate the effectiveness and limitation of GWT.

3.2.1 Two Gaussian Atoms

In this example a signal composed of two Gaussian atoms is being considered. Its t-f representations are shown in Fig 3.1. GT clearly shows two Gaussian atoms but its t-f representation is blurred with poor concentration of energy. Whereas, WD clearly gives good energy concentration for Gaussian atoms. However, we wrongly see third Gaussian atom appearing in between original two components. GWT shows signal components with same energy concentration as that of WD with CT completely eliminated.

3.2.2 Three Gaussian Atoms

In this example a signal composed of three Gaussian atoms is being considered. Its t-f representations are shown in Fig 3.2. GT shows blurred t-f representation of Gaussian atoms. WD clearly gives good energy concentration for Gaussian atoms. However, we wrongly see two extra Gaussian atoms due to CT. GWT eliminates CT and gives crisp representation for lower most and upper most Gaussian atom, but the Gaussian atom appearing in center still suffers from CT because of overlapping of CT of WD on its auto-term region.

3.2.3 Parabolic Chirp

In this example a parabolic chirp is being considered. It t-f representations are shown in Fig 3.3. GT gives blurred representation of signal. WD suffers from

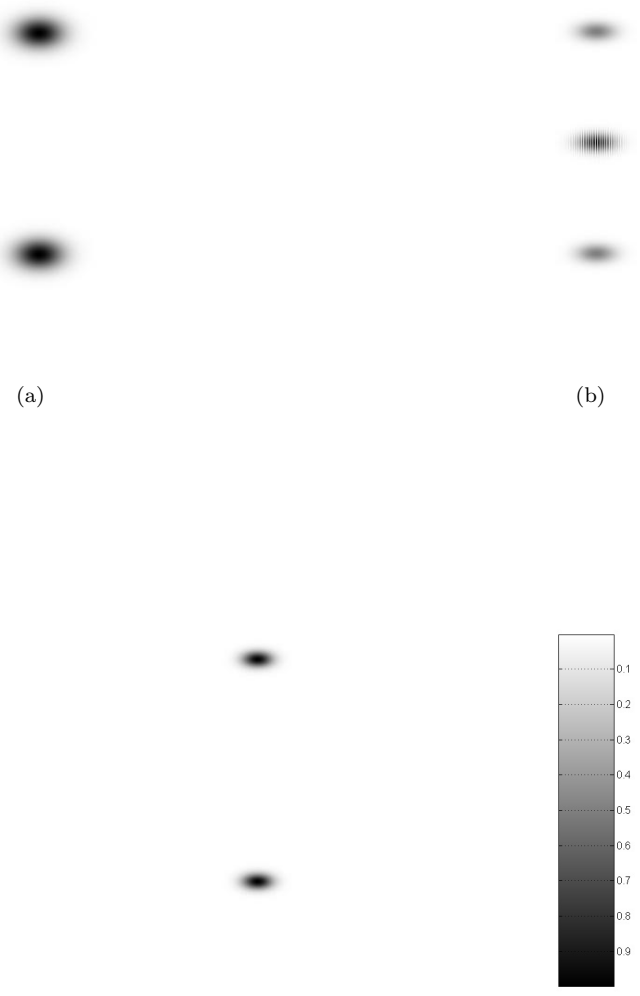

(a) (b)

(c)

FIGURE 3.1: (a) GT (b) WD (c) GWT

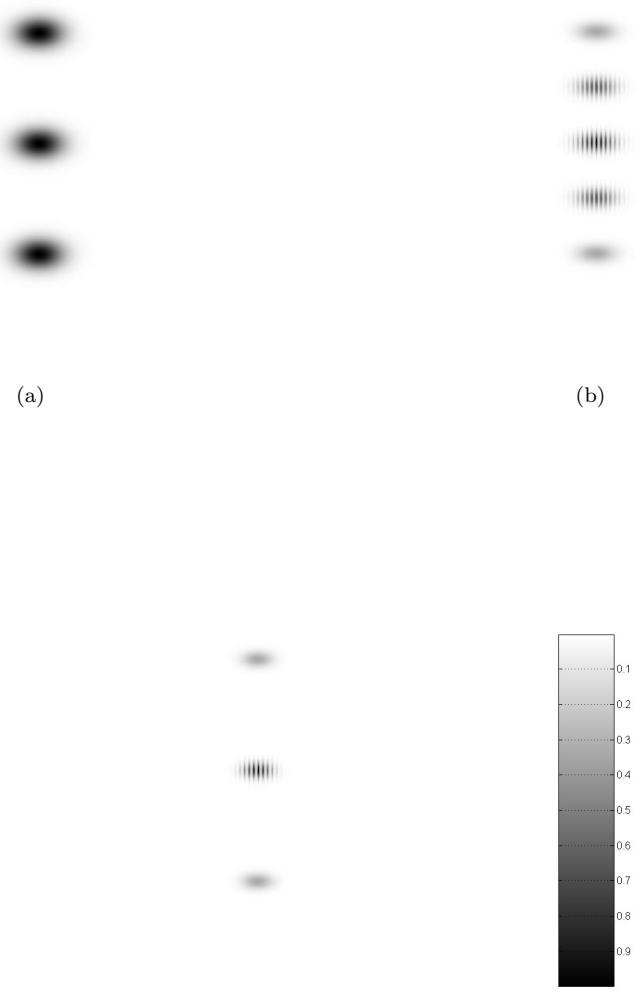

(a) (b)

(c)

FIGURE 3.2: (a) GT (b) WD (c) GWT

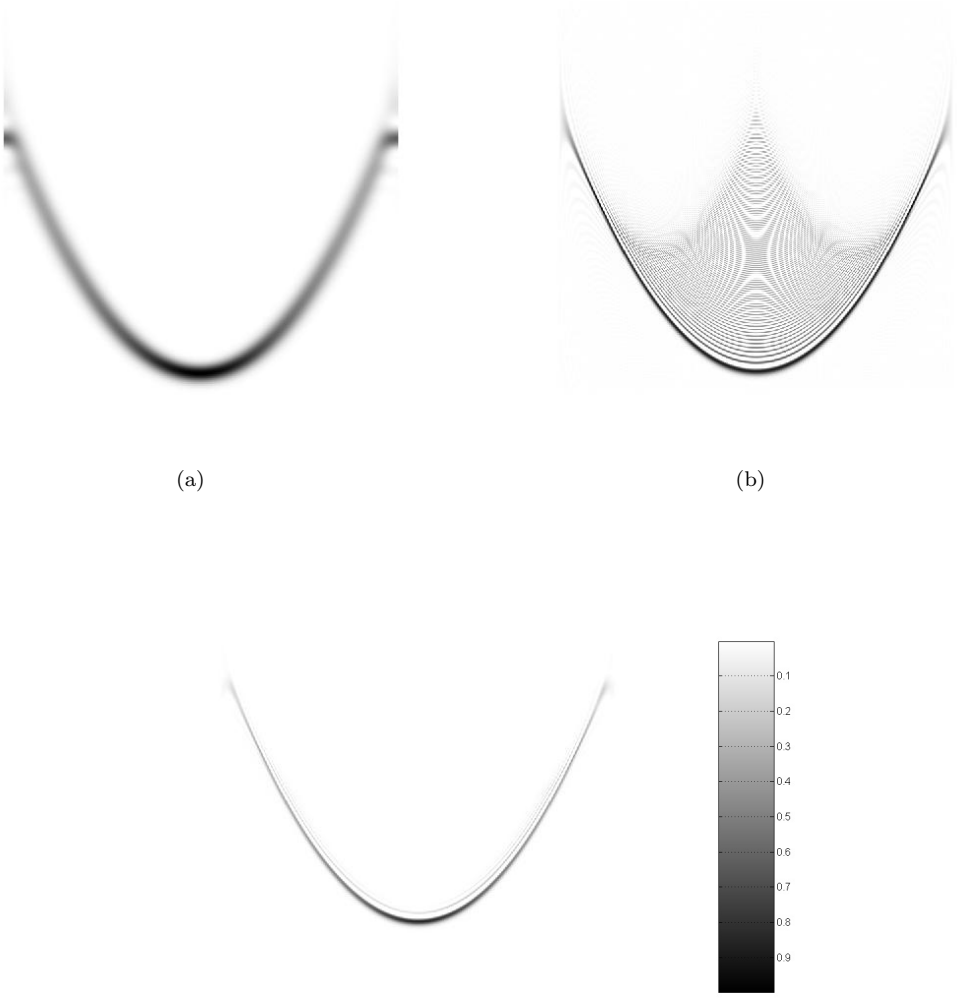

(a) (b)

(c)

FIGURE 3.3: (a) GT (b) WD (c) GWT

inner interference. GWT suppresses inner interference terms to large extent and gives crisp representation. This property of GWT to suppress inner interference will be exploited in next chapter to remove the CT of mono-component filtered signal components.

Chapter 4

CROSS-TERM SUPPRESSION USING 2D SIGNAL PROCESSING TECHNIQUES

An efficient method based on 2D Signal processing techniques and fractional Fourier transform is presented to suppress interference terms of WD. A part of this chapter has been published in Khan et al. (2011). The proposed technique computes GT of a multi-component signal to obtain a blurred t-f image. Signal components in GT image are segmented using connected component segmentation and are filtered out using precise application of FrFT. A crisp t-f representation is then obtained by computing sum of products of WD and GT of the isolated signal components. The efficacy of the proposed technique is demonstrated using example of synthetic signal. Proposed scheme gives satisfactory performance even when CT of WD overlap auto-terms and computational cost analysis shows that it is more efficient than recent interference suppression techniques of comparable performance. Moreover, proposed technique does not require any prior information regarding nature of signal. Block diagram of the proposed technique is given in Fig 4.1.

Rest of the chapter is organized as follows. Section 4.1 presents the theoretical background related to present work and the problem formulation. The proposed hybrid approach to obtain a crisp t-f representation is illustrated in section 4.2 giving details of the algorithmic steps. Step by step demonstration of the proposed scheme is given in section 4.3. Computational cost of the proposed scheme is presented in 4.4. Finally section **??** discusses the mathematical properties of the proposed scheme.

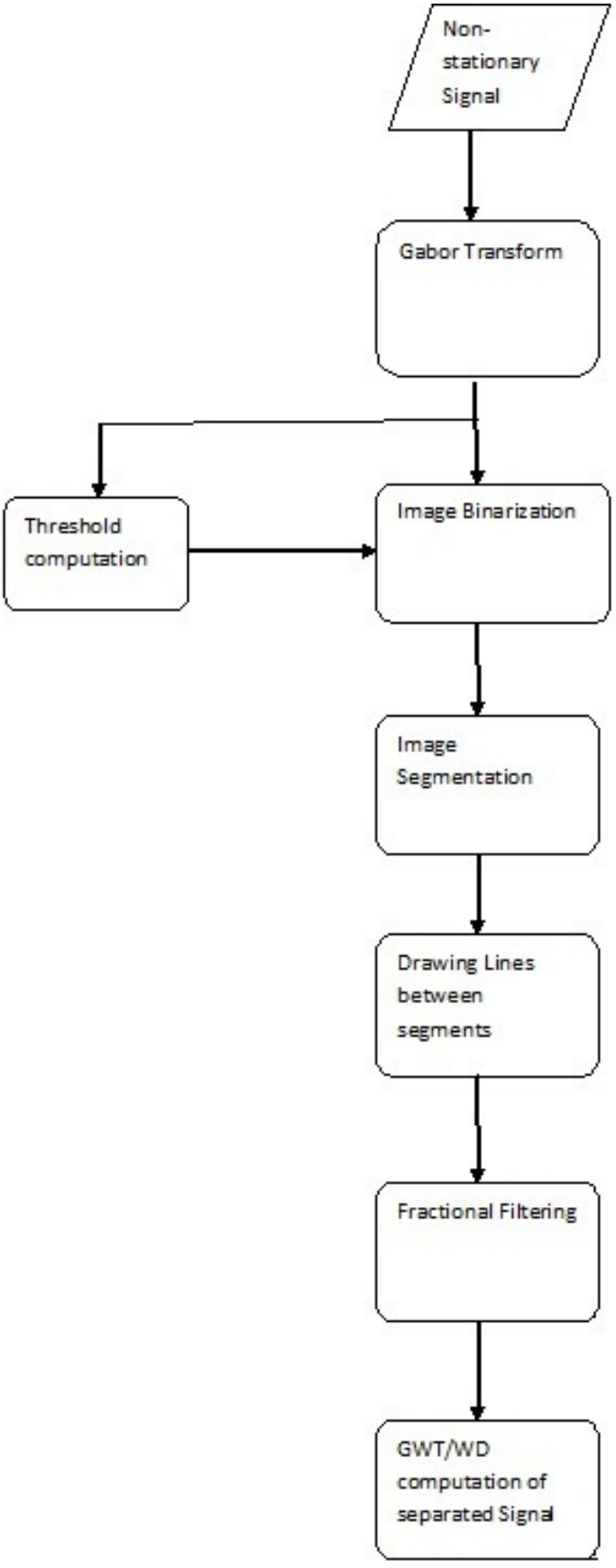

FIGURE 4.1: Block Diagram representation of Proposed technique

4.1 Problem Formulation

The technique presented in this study involves selective application of fractional filtering to achieve the WD with significantly reduced CT. This section gives an overview of the problem at hand and an abstract description of solution to the problem with its mathematical justification. Following subsections discuss the desired t-f distribution, Support Vector Machine (SVM), and describe FrFT as a tool to perform time-varying filtering.

4.1.1 Desired time frequency representation

Applicability of WD is severely restricted by the presence of the unwanted CT. Direct computation of WD would result in unwanted interference terms as discussed in chapter 2 and 3. However, desired t-f representation should only have the auto-terms of the WD. Mathematically,

$$D(t,\omega) = \sum_{i=1}^{N} WD_{s_i s_i}(t,\omega). \qquad \textit{Eq (4.1)}$$

The t-f distribution composed only of the auto-terms of WD would give ideal t-f distribution for linearly frequency modulated signals. However, for nonlinear frequency modulation of signal components, the proposed t-f representation would still have the CT. These CT arising due to nonlinear nature of frequency modulation can be suppressed by computing GWT of the signal components as demonstrated in chapter 3. Thus for the signals composed of non-linearly frequency modulated components, the desired t-f distribution would be as follows,

$$D(t,\omega) = \sum_{i=1}^{N} GWT_{s_i}(t,\omega), \qquad \textit{Eq (4.2)}$$

$D(t,\omega)$ can be computed by separating signal components and then calculating WD/GWT of isolated signal components and finally adding up the individual GWT/WD.

4.1.2 Support Vector Machines

SVM Hsu et al. (2003) is a powerful tool used for the purpose of classification in signal processing applications. In this study, we have used SVM to draw a separating boundary between different segments in a t-f plane. Consider a set of points of the form.

$$D = ((x_i, c_i)|x_i \in R^2, c_i \in -1, 1)_{i=1}^{n}, \qquad Eq\ (4.3)$$

where the c_i is either 1 or -1, indicating the segment to which the point belongs. Each x_i is a 2-dimensional vector representing a pixel belonging to image segment in t-f plane. We want to find the line which gives the maximum margin between the points having $c_i = 1$ and those having $c_i = -1$. Two lines parallel to the optimal separating line are drawn such that both the lines separate the data. Mathematically,

$$w.x - b = 1 \quad \text{and} \quad w.x - b = -1. \qquad Eq\ (4.4)$$

Thus the problem of finding the optimal separating line is reduced to minimizing the objective function $\frac{1}{2}|w|^2$ subject to the constraint $c_i(w.x_i - b) \geq 1$. This problem can be solved by quadratic programming techniques Hsu et al. (2003).

4.1.3 Fractional Fourier Transform

The proposed technique for computing the desired t-f representation is based on the separating signal components and analyzing them separately using WD. The signal components that overlap in both time and frequency domains cannot be separated by any stationary band-pass filter. FrFT has emerged as a powerful tool for separating the time-varying signals that are linearly separable in the joint t-f plane. Mathematically, an α order FrFT is defined as Namias (1980),

$$s_\alpha(u) = \int B_\alpha(u,t)s(t)dt, \qquad Eq\ (4.5)$$

$$B_\alpha(u,t) = \frac{e^{-j\pi\frac{sgn(\phi)}{4}+j\frac{\phi}{2}}}{|sin\phi|^{\frac{1}{2}}} e^{j\pi(u_2 cot\phi - 2utcsc\phi + t^2 cot\phi)}. \qquad Eq\ (4.6)$$

Here $\phi = \alpha\frac{\pi}{2}$. As shown in previous studies by Mustard (1996), the WD of $s_\alpha(u)$ is the rotated version of WD of original signal by angle α. Mathematically,

$$WD_{s_\alpha}(t,\omega) = R_{-\alpha}(WD_s(t,\omega)). \qquad Eq\ (4.7)$$

R_α is an operator that rotates a joint t-f plane clock wise. Signal components that are linearly separable in joint t-f plane can be separated by using the following steps as demonstrated by Arikan and Kemal Ozdemir (2000) and Pei and Ding (2007).

- First compute α order FrFT of signal, i.e. rotate the signal components in t-f plane.
- Apply band pass filters to separate signal components.
- Finally, compute -ive α order FrFT, i.e. inversely rotate the signal components in t-f plane.

In order to elaborate above mentioned procedure, consider Fig 4.2(a) showing the joint t-f representations of a signal composed of two linear chirps. It is clear from these representations that the signal components overlap in both time and frequency domains. Thus they cannot be separated by any standard filtering technique. However, if we rotate the t-f representation of the given signal by computing its FrFT as shown in Fig 4.2(b) then these components can easily be filtered by any standard band-pass filter. Fig 4.2(c) and Fig 4.2(d) shows the t-f signal components separated by a band-pass filter in fractional Fourier domain.

Finally, the -ive α order FrFT of filtered signal components is computed to obtain the original signal components, as shown in Fig 4.2(e) and Fig 4.2(f).

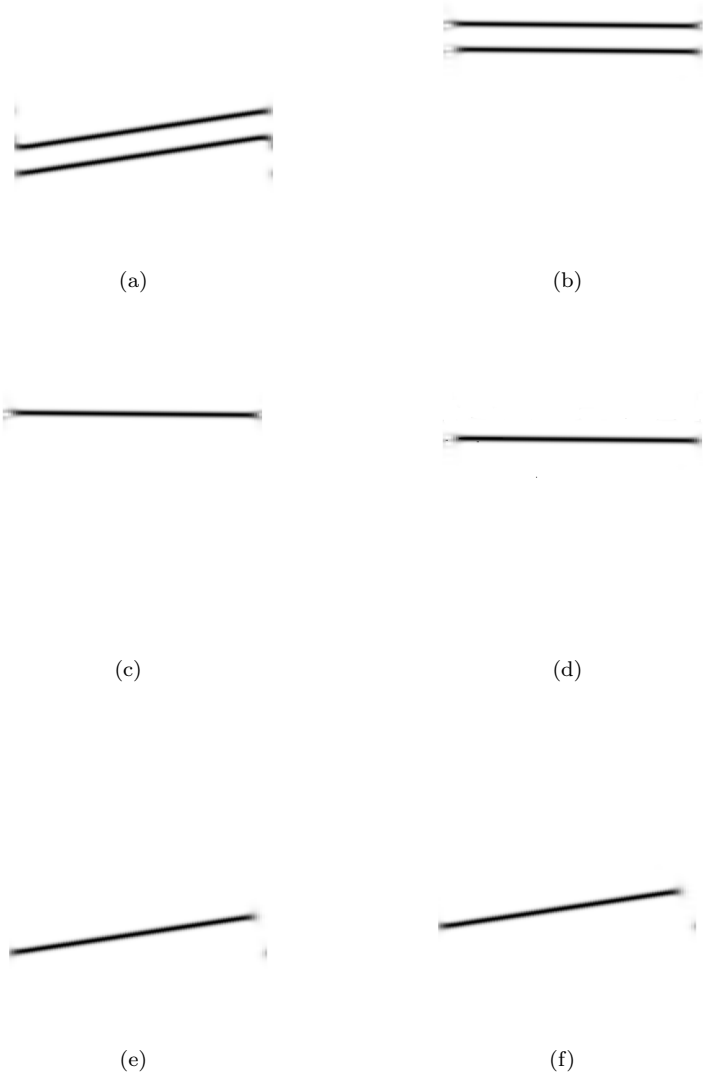

FIGURE 4.2: (a) GT (b) GT of FrFT of signal (c) GT of separated signal component in fractional domain (e) GT of separated signal component in fractional domain (f) GT of separated signal component (g) GT of separated signal component

In the following section, fractional filters are applied to isolate the signal component that are linearly separable or piecewise linearly separable in t-f plane.

4.2 The Proposed Approach

This section presents a hybrid image processing and fractional Fourier technique to compute the WD with significantly reduced CT. The proposed approach isolates each signal component and analyzes the isolated components separately using GWT. A blurred t-f image is obtained by computing the GT image of multi-component signal. The GT image is segmented using an 8-connectivity criterion. Each connected segment S_i in t-f plane corresponds to the individual signal components $s_i(t)$ in time domain. The parameters of the separating line segments drawn between segments define the order of fractional filters used to isolate signal components. As discussed in previous sections, the isolated signal components can be analyzed by computing their GWT or WD. Major steps of the proposed approach are:

4.2.1 Blurred time frequency representation

The blurred t-f representation is obtained by computing GT of multi-component signal $s(t)$. The purpose of this step is to locate signal components in t-f plane.

4.2.2 Image thresholding

GT image formed in earlier consists of foreground and background regions. Foreground represents the region in t-f plane where signal is present. Whereas, background represents the regions in t-f plane where signal is not present. Foreground and background regions can be identified by converting the t-f intensity image into a binary image by the application of a thresholding process given by,

$$B(t,\omega) = 0, \quad \text{if} \quad GT(t,\omega) \geq T, \qquad \textit{Eq (4.8)}$$

$$B(t,\omega) = 1, \quad \text{if} \quad GT(t,\omega) < T, \qquad \textit{Eq (4.9)}$$

where T is a threshold that is adaptively selected using the following iterative algorithm as discussed by Acharya and Ray (2005):

1. Initially the mean value of the GT image is selected as a threshold T.
2. In each iteration,
   - All pixels having value greater then a threshold 'T' are stored in image IA and values less than a threshold are stored in image IB. Mathematically,

$$IA(t,\omega) = GT(t,\omega), \quad \text{if} \quad GT(t,\omega) \geq T \qquad Eq\ (4.10)$$

$$IA(t,\omega) = 0, \quad \text{else where} \qquad Eq\ (4.11)$$

$$IB(t,\omega) = GT(t,\omega), \quad \text{if} \quad GT(t,\omega) < T \qquad Eq\ (4.12)$$

$$IB(t,\omega) = 0, \quad \text{else where} \qquad Eq\ (4.13)$$

   - New threshold is computed by taking average of the respective means of IA and IB. Mathematically,

$$T = \frac{u_{IA} + u_{IB}}{2}. \qquad Eq\ (4.14)$$

3. Steps 2 is repeated and the threshold T is updated in each iteration. The iterations are terminated when the threshold value does not change in two successive iterations.

4.2.3 Image Segmentation

The purpose of image segmentation is to decompose the foreground of the t-f image into non-overlapping regions representing signal components. It is assumed that all signal components have non-overlapping t-f signatures. Therefore, the binary t-f image of a multi-component signal having N number of components can be

decomposed into N foreground segments and one background region. Mathematically,

$$B = \bigcup_{i=1}^{N} S_i \bigcup B_0, \qquad \textit{Eq (4.15)}$$

where B is a set containing all foreground and background pixels of a binary image, S_i is the set of pixels representing $s_i(t)$ in time domain, and B_0 is the set of pixels representing background. All the pixels in each segment must fulfill the connectivity criterion that is stated for each pixel as follows. A pixel belonging to a segment must have at least one other pixel of the same segment in its 8-neighborhood and it should not have any pixel of any other segment in its 8 neighbors. 8-neighborhood of a pixel at the location (x, y) is defined as a set of all pixels at the following locations,
$(x-1, y)(x+1, y)(x-1, y-1)(x+1, y+1)(x-1, y+1)(x+1, y)(x+1, y-1)(x, y+1)(x, y-1)$.

Further details of the algorithm for image segmentation based on connectivity criteria are given by Acharya and Ray (2005).

In order to illustrate the steps of image segmentation algorithm, consider the t-f representation of a signal composed of two parabolic chirps as shown in Fig 4.3. The t-f image is thresholded first and then segmented into two different sets by using connectivity criteria shown in different colors.

4.2.4 Drawing separating boundaries between regions

In the previous section, it was discussed that fractional filters can be used for separating the signal components that are linearly separable in t-f domain. In order to apply fractional filters, we need to compute the order of these filters, i.e. rotation order and cut-off. These two parameters can be evaluated from the parameters, i.e. slope and location of separating lines between segments. In order to find the optimum separating line between any two segments, we use SVM as

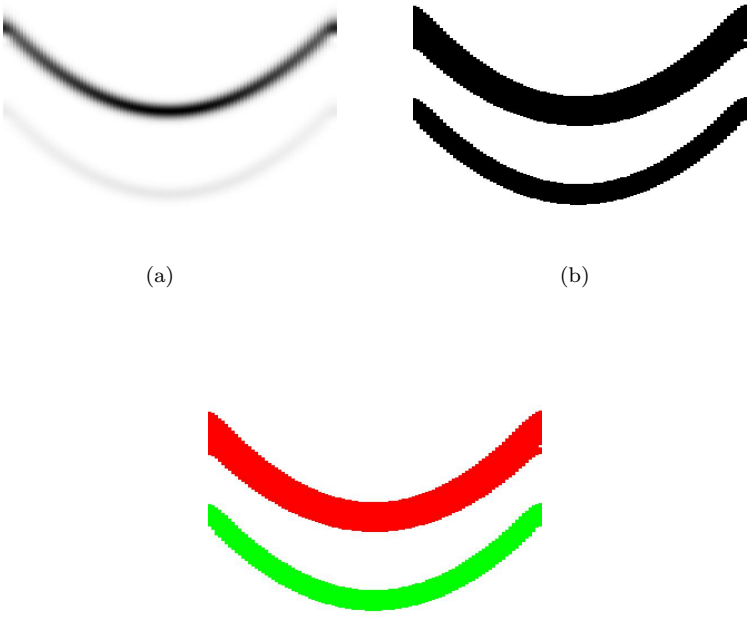

(a) (b)

(c)

FIGURE 4.3: (a) GT (b) Binary Image (c) Segmented Image

discussed in the previous section. We have used linear primal SVM algorithm because of its computational efficiency as discussed by Chapelle (2007). For each segment S_i, J_i number of lines $l_{ji}(x_{sji}, y_{sji}, x_{eji}, y_{eji})$ are drawn to separate S_i from the regions that are above S_i in t-f plane. $(x_{sji}, y_{sji}, x_{eji}, y_{eji})$ are the starting and ending points of the jth line drawn for segment S_i. The total number of lines drawn depends upon whether the segments are linearly separable or not. If they are linearly separable, only one line would be enough. However, for nonlinearly separable segments, multiple straight lines need to be drawn. Initially SVM is used to draw the best possible straight line between two segments. If a drawn line intersects S_i or segments above, then S_i is split into two sub-regions and lines are drawn for both sub-regions. This process is recursively repeated till all the regions are separated by lines.

In order to give step by step illustration of the proposed algorithm for drawing

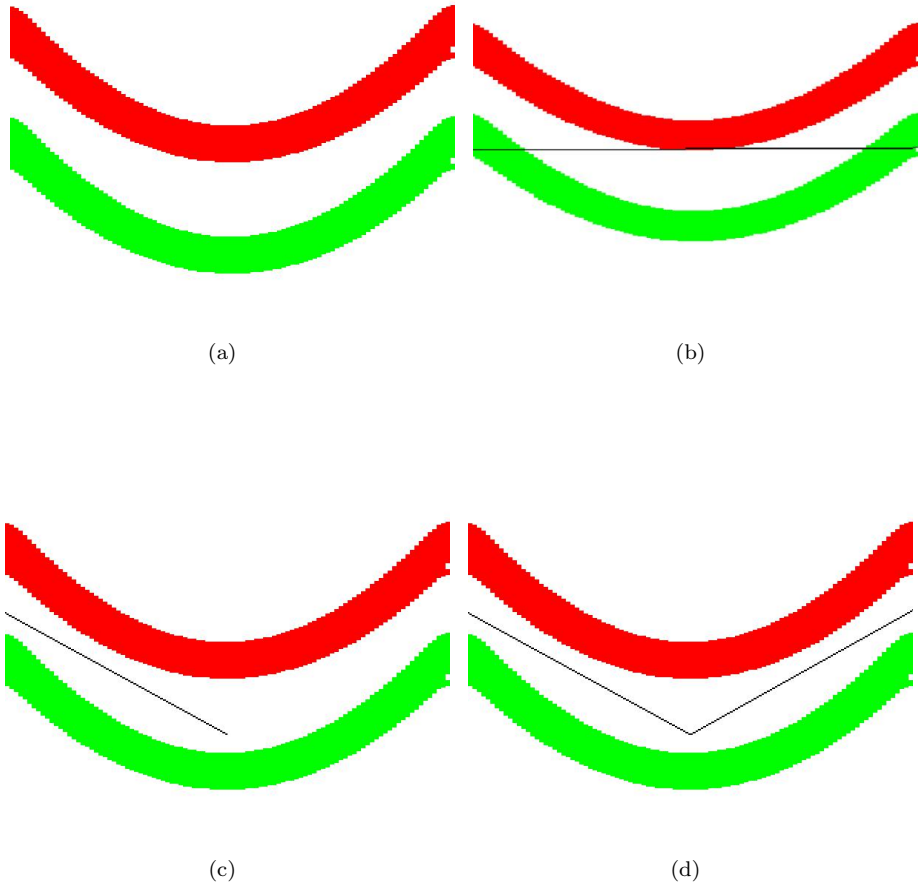

FIGURE 4.4: (a) Segmented Image (b) Segments separated by drawing horizontal line (c) Sub Segments separated by drawing line (d) Segment separated by multiple lines

the separating lines, a segmented t-f image of a signal composed of two parabolic chirps is considered as shown in Fig 4.4(a). The t-f signature of different signal components is labeled by using different colors. SVM is used to draw a single line between these two segments. The drawn line intersects both segments as shown in Fig 4.4(b); therefore, a single line is insufficient and fails to separate the two segments. Thus, the segments are divided into two sub-regions and the lines are drawn for each of them as shown in Fig 4.4(c) and Fig 4.4(d).

4.2.5 Fractional Filtering

Each signal component appearing as segment S_i in t-f plane is filtered out using following procedure.

- Signal $s[n]$, obtained by sampling of signal, is decomposed into J_i smaller signals corresponding to lines l_{ji}.

$$s[n] = \sum_{j=0}^{J_i} \widehat{s}_{ji}[n], \qquad \textit{Eq (4.16)}$$

where J_i is the total number of lines separating S_i from other segments in t-f plane that are above $s_i(t)$ in t-f plane.

$$\widehat{s}_{ji}[n] = s[n], \quad \text{for} \quad x_{sji} \leq n < x_{eji} \qquad \textit{Eq (4.17)}$$

$$\widehat{s}_{ji}[n] = 0. \quad \text{else where} \qquad \textit{Eq (4.18)}$$

$TF_{\widehat{s}_{ji}}(n,l)$ that is the t-f representation of decomposed signal $\widehat{s_{ji}}[n]$, can be related to $TF_{\widehat{s}}(n,l)$, the t-f representation of $s[n]$, by the following equation.

$$TF_{\widehat{s}_{ji}}(n,l) = \sum_{k=0}^{N_s-1} TF_s(n,k) sinc((\frac{N_s l}{x_{eji} - x_{sji}}) - k) \text{ for } x_{sji} < n < x_{eji}, 0 < l < x_{eji} - x_{sji}. \qquad \textit{Eq (4.19)}$$

Here N_s is the length of signal $s[n]$. Above equation clearly shows that t-f representation of the decomposed signal gets scaled along frequency axis by the factor of $\frac{x_{eji}-x_{sji}}{N_s}$ as a result of signal decomposition. This effect is demonstrated in Fig 4.5. Fig 4.5(a) shows t-f representation of a signal composed of two quadratic chirps with signal duration from -1.5s to 1.5s while Figure 4.5(b) shows t-f representation of same signal, but time duration limited to -1.5s to 0s. This scaling also affects the slope of separating line drawn between segmented images corresponding to two chirps as shown in Fig 4.5(c) and Fig 4.5(d) respectively.

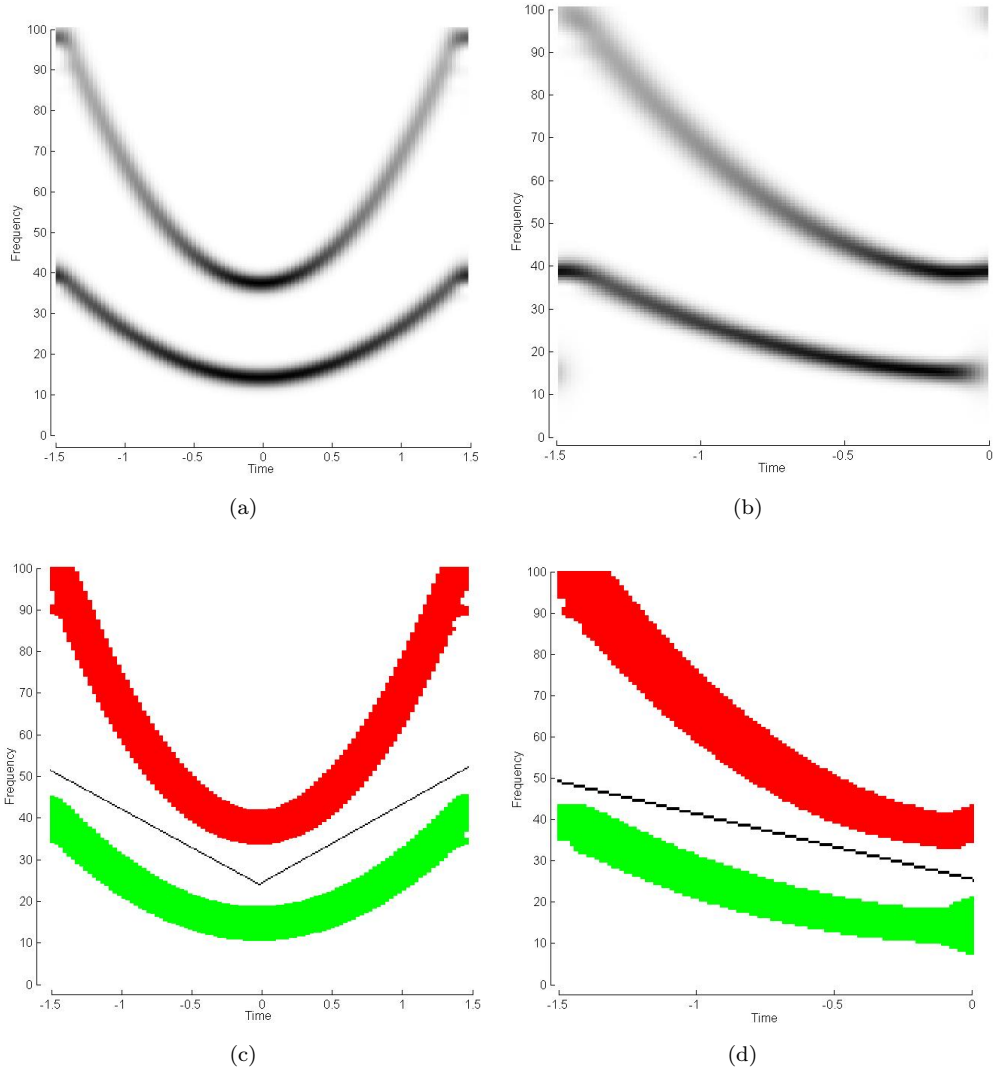

FIGURE 4.5: (a) GT of two quadratic chirps (b) GT of only half portion of quadratic chirps (c) Segmented GT image of two quadratic chirps with segments separated by lines drawn (e) Segmented GT image of only half portion of quadratic chirps with lines drawn

- Fractional filters are applied to separate decomposed signals $\widehat{s}_{ji}[n]$ from all those signal components that are above segment S_i in t-f plane thus forming low-pass signals $\widehat{s}_{lji}[n]$. we have used ideal low pass filters for this purpose. Order of fractional filters that is rotation order α_{ji} and frequency cut-off ω_{ji} can be estimated from the slope and y-intercept of separating lines drawn. Scaling of frequency axis of t-f representation of the decomposed by the factor of $\frac{(x_{eji}-x_{sji})}{N_s}$ also scales the slopes of the separating lines by the same

factor as shown in Fig 4.5. Thus, the rotation order would be

$$\alpha_{ji} = \frac{2}{\pi} tan^{-1}(\frac{m_{ji}(x_{eji} - x_{sji})}{N_s}). \qquad Eq\ (4.20)$$

Here m_{ji} is the slope of line l_{ji} and is given by

$$m_{ji} = \frac{y_{eji} - y_{sji}}{x_{eji} - x_{sji}}. \qquad Eq\ (4.21)$$

The frequency cut-off is computed from the y-intercept of the separating line. Mathematically,

$$\omega_{ji} = \pi \frac{y_{eji} + y_{sji}}{N_s}. \qquad Eq\ (4.22)$$

- The decomposed, low-pass filtered signal components $\widehat{s}_{lji}$ are finally added up to form a "low pass" signal s_{li}.

$$s_{li}[n] = \sum_{j=1}^{J_i} s_{lji}[n]. \qquad Eq\ (4.23)$$

- As a result of above mentioned steps, $s_{li}[n]$ is separated from all the components that have segments above S_i in the t-f plane, and it is composed of $s_i[n]$ and all the components that have segments that appear below S_i in t-f plane. Similar procedure is repeated with $s_{li}[n]$ as an input signal to separate $s_i[n]$ from all the signal components that have segments below S_i in t-f plane.

4.2.6 Computing GWT or WD of isolated signal components

GWT or WD of the isolated and filtered signal components is calculated. Choice of whether to compute WD or GWT depends upon application at hand. If the given signal is composed of just linear chirp components, then only WD should be calculated. However, for signals composed of non-linearly frequency modulated chirps, GWT would be a better choice as demonstrated in Fig 3.3. GWT of the

isolated signal is normalized by the maximum value of WD to preserve signal relative amplitudes in t-f representation. Mathematically,

$$GWT_{s_i}(t,\omega) = \frac{WD_{s_i}(t,\omega)GT_{s_i}(t,\omega)}{WD_i^{max}}, \qquad Eq\ (4.24)$$

where WD_i^{max} is the maximum value in WD of isolated signal component $s_i(t)$. Finally, the GWTs/WDs of all the separated signal components are added up to obtain suppressed interference crisp t-f representation.

4.3 Step By Step Demonstration

Signal composed of three parabolic chirps with varying amplitudes is considered in this example, defined by following equation,

$$s(t) = e^{-j(20\pi t^3+76\pi t)} + 0.8e^{-j(8\pi t^3+50\pi t)} + 0.6e^{-j(8\pi t^3+10\pi t)}. \qquad Eq\ (4.25)$$

The sampling frequency is chosen to be 200Hz and the signal duration is taken to be from -1.5s to 1.5s. A step by step illustration of the proposed scheme is shown in Fig 4.6. WD of the given signal is shown in Fig 4.6(a), GT in Fig 4.6(b), and GWT in 4.6(c). Result of image segmentation is shown in color image Fig 4.6(d). Different components are shown in different colors. Fig 4.6(e) shows segments separated by lines. Fig 4.6(f), Fig 4.6(g), Fig 4.6(h) shows the WDs of filtered signal components. Finally, the desired t-f representation is obtained by adding GWTs of separated signal component as shown in Fig 4.6(i). Fig 4.6 clearly reveals that the proposed technique outperforms GT, WD and GWT. GT image gives blurred t-f representation. Whereas, WD is hardly readable due to interference of the CT. GWT overcomes limitation of GT and WD to an extent. GWT gives the de-blurred and the CT free representation of lower most chirp but upper two chirps still suffer from CT. The proposed t-f representation overcomes the limitation of all three techniques. The proposed t-f representation clearly resolves all three chirps and it does not suffer from CT interference problem.

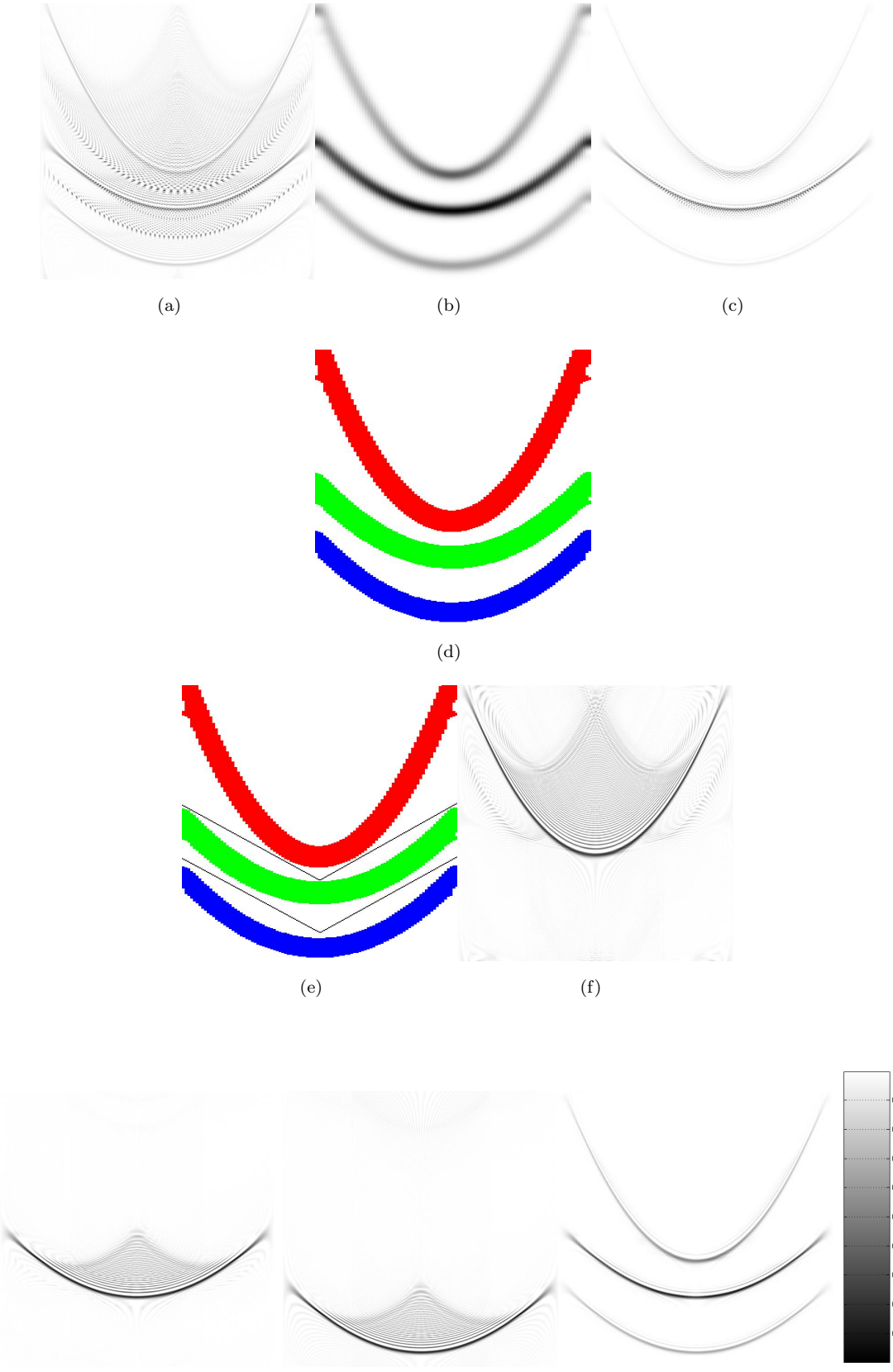

FIGURE 4.6: (a) WD (b) GT (c) GWT (d) GT Segmented (e) Segmented image with Lines drawn (f) WD of isolated signal (g) WD of isolated signal (h) WD of isolated signal (i) The Proposed Approach

4.4 Computational Cost Analysis

It is clear from the example considered that the proposed technique results in almost CT free t-f representation in which quality of auto-terms in not compromised. Unlike GWT or kernel based methods, this technique performs well even in scenarios when the auto-terms of WD of a signal overlap the CT. This improvement comes at the expense of increased computational cost. Computational cost of the proposed algorithm is equal to sum of computational cost of the GT image computation, image segmentation, drawing the separating boundaries, fractional filtering and computing GWT of the separated components. The computational cost of the GT image computation is $O(N_s^2 log(N_s))$, that of image segmentation is $O(N_s^2)$ as given by Acharya and Ray (2005), and that of fractional filtering is $O(N_s log(N_s))$. In order to make the proposed scheme computationally efficient, the primal form of SVM presented by Chapelle (2007) with computational cost of $O(N_s d^2 + d^3)$ is used. Here d is the number of dimensions, which in this case are equal to two. The computational cost of a single computation of GWT is $O(N_s^2 log(N_s))$ as it involves computation of the product of WD and GT. There are N number of components in signal. Thus, the total computational cost of the proposed algorithm is $O(N(2N_s^2 log(N_s) + N_s log(N_s) + N_s^2 + N_s) + N_s^2 log(N_s))$or simply $O(NN_s^2 log(N_s))$. In the analysis of these algorithms, computational cost of higher order is considered and constants are ignored as is the general practice. The computational cost of the proposed technique depends upon two variables, namely, the number of samples in signal, and the number of components in signal. Unlike the computational cost of GWT or other kernel based methods whose computational cost is independent of number of components in signal, computational cost of the proposed scheme increases linearly with number of components as shown in Fig 4.7.

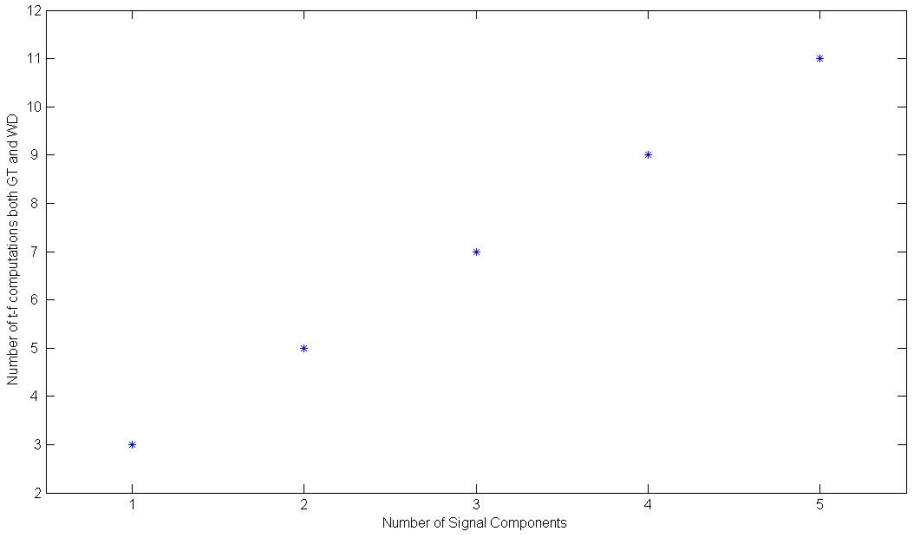

FIGURE 4.7: Computational cost vs number of signal components

4.5 Mathematical Properties of the Proposed t-f distribution

The proposed t-f distribution is designed with the objective to reduce the CT of WD and it cannot be strictly called a WD. CT contain part of signal energy. Therefore, their removal effects the mathematical properties of reultant t-f distribution. The proposed t-f distibution does not fulfill mathematical properties of WD that are related to signal energy like time and frequency marginals. However, rest of the mathematical properties of WD like time shift, frequency shift, time support, frequency support, IF, and group delay are still preserved.

Chapter 5

PERFORMANCE ANALYSIS OF THE PROPOSED TECHNIQUE

In this chapter, we compare the proposed technique with other standard techniques proposed in the literature on the basis of following criterion:

1. Energy concentration
2. CT suppression
3. Resolution
4. Readability

The proposed technique processes GT for identification of signal components, therefore, it suffers from same resolution limitation as that of GT. However, the proposed technique demonstrates good energy concentration property. Therefore, the performance of proposed technique will be evaluated on the basis of energy concentration, CT suppression and readability criteria.

Energy concentration and CT suppression of a t-f representation can be evaluated both visually and on the basis of quantitative measures, such as, ratio of norms by Jones and Parks (1992), Shannon entropy measure by Shannon (2001), normalized Renyi Entropy measure by Sang and Williams (1995), LJubisa measure by Stanković (2001). These Readability of t-f representation is a subjective criteria and can only be judged on the basis of visual interpretation.

Rest of the chapter is organized as follows. Quantitative measures employed for comparing t-f distributions is discussed in section 5.1. These quantitative measures are discussed in detail by Boashash (2003). The performance of the proposed technique, on the basis of visual inspection and quantitative measures versus other

standard techniques, is presented in section 5.2. In section 5.3 comparison of the proposed technique with the techniques of similar performance is made on the basis of readability and computational cost. Section 5.4 summarizes the chapter.

5.1 Quantitative measures

Quantitative measures employed for comparing t-f representations are based on entropy and energy criteria. Entropy is a quantitative measure used for computing information. In the context of t-f representation higher entropy implies more blurring, CT and less energy concentration. Whereas, less entropy implies that given t-f representation is more concentrated and has lesser CT. Same analogy goes for energy based t-f representations. T-f representation with less energy implies more energy concentration and better suppression of CT.

5.1.1 Shannon Entropy

Shannon criteria for t-f representation can be mathematically expressed as

$$E_{shannon} = \sum_{n} \sum_{\omega} Q(n,\omega) log_2(Q(n,\omega)). \qquad Eq\ (5.1)$$

It is assumed that $E_{shannon}$ has a unit energy. Mathematically,

$$\sum_{n} \sum_{\omega} Q(n,\omega) = 1. \qquad Eq\ (5.2)$$

However, above mentioned equation cannot be applied for t-f representation with negative values. Therefore, in such scenarios absolute values may be used. Mathematically,

$$E_{shannon} = \sum_{n} \sum_{\omega} |Q(n,\omega)| log_2(|Q(n,\omega)|) \qquad Eq\ (5.3)$$

However, using absolute values will increase the overall energy of distribution which may assume negative values like WD.

5.1.2 Renyi Entropy

In order to overcome the limitation of Shannon entropy for dealing with distributions with negative values Renyi entropy can be employed. Mathematically,

$$E_{Renyi} = \frac{1}{1-\alpha} log_2(\sum_n \sum_\omega Q^\alpha(n,\omega)), \qquad Eq\ (5.4)$$

where α is the order of entropy. We have taken its value to be equal to 3. In order to make the above mentioned measure energy unbiased, we consider a normalized entropy measure.

$$E_{Renyi} = \frac{1}{1-\alpha} log_2(\frac{\sum_n \sum_\omega Q^\alpha(n,\omega)}{\sum_n \sum_\omega Q(n,\omega)}) \qquad Eq\ (5.5)$$

5.1.3 Ratio of Norms

Jones and Parks (1992) presented a measure of energy concentration based on ratio of norms. Mathematically,

$$E_{jp} = \frac{\sum_n \sum_\omega |Q(n,\omega)|^4}{(\sum_n \sum_\omega |Q(n,\omega)|^2)^2} \qquad Eq\ (5.6)$$

Unlike entropy based criterion, higher value of E_{jp} implies better energy concentration

5.1.4 Ljubisa Measure

Stanković (2001) proposed a criterion for assessment of energy concentration of time limited signals. Mathematically,

$$J[Q(n,\omega)] = (\sum_n \sum_\omega |Q(n,\omega)^{\frac{1}{\beta}}|)^\beta, \qquad Eq\ (5.7)$$

where

$$\sum_n \sum_\omega Q(n,\omega) = 1 \qquad Eq\ (5.8)$$

and $\beta > 1$. The t-f representation that minimizes $J[Q(n,\omega)]$ is assumed to be the best distribution.

5.2 Performance Evaluation of the Proposed Technique

In order to compare the performance of proposed technique, based on energy criterion established in earlier section, we consider four synthetic and one real life test signal. Performance of the proposed technique is compared with GT, WD, Pseudo Wigner Distribution (PWD), GWT, PAGE and Zhao-Atlas-Marks distribution(ZAM) .

5.2.1 Four linear chirps

A simple signal composed of four linear chirps is being considered. For comparison signal is analyzed by various t-f distributions as shown in Fig 5.1. GT gives CT free but blurred representation, both WD and PWD suffer from severe CT interference problem and we wrongly see 6 extra chirps, ZAM fails to resolve signal components, and GWT gives clear and crisp representation, but it wrongly displays one extra chirp in t-f plane. This extra chirp appeared because of overlapping of CT of WD in the support regions of GT. The proposed t-f representation clearly displays all the four chirps. This fact is also verified by quantitative analysis. The proposed scheme has minimum value for all entropy based measures and has maximum value for ratio of norms as shown in table 5.1.

5.2.2 Linear chirp, Gaussian atom and parabolic chirp

A simple signal composed of linear chirp, Gaussian atom and parabolic chirp is being considered. For comparison signal is analyzed by various t-f distributions as shown in Fig 5.2. GT gives CT free but blurred representation, WD suffers from both inner interference and outer interference, inner interference is suppressed to

TABLE 5.1: 4 Linear Chirps

T-F Representation	Shannon	Renyi	Ratio of Norms	Ljubisa
PAGE	17.51	16.52	0.0221	0.6815
PWD	16.2731	15.29	0.0454	0.2445
ZAM	17.54	16.82	0.0136	1.37
GT	16.51	15.97	0.0215	0.54
GWT	14.78	12.93	0.3773	0.0205
The Proposed Approach	13.78	12.34	0.4308	0.0073
WD	16.78	14.30	0.2306	0.1093

large extent in PWD, but it still suffers from outer interference, PAGE distribution is hardly readable, ZAM suppresses both inner and outer interference to large extent but auto-terms also get blurred, and GWT suppresses CT to large extent but CT still corrupt the auto-terms in regions where CT of WD overlap auto-terms. The proposed technique gives crisp and almost CT free t-f representation in which all signal components can be seen clearly with their relative amplitudes preserved. This fact is also verified from quantitative analysis. It can be seen that all entropy based measures are minimum and ratio of norms has second largest value for the proposed approach as shown in table 5.2.

TABLE 5.2: Linear, Quadratic Chirp And Gaussian Atom

T-F Representation	Shannon	Renyi	Ratio of Norms	Ljubisa
PAGE	17.1548	15.8730	0.0441	2.2643
PWD	15.8551	14.5638	0.0840	1.0838
ZAM	16.5798	14.1299	0.3270	0.9994
GT	15.7986	14.9353	0.0589	1.0547
GWT	14.6161	13.2483	0.2502	0.1441
The Proposed Approach	13.7250	12.6326	0.3159	0.0607
WD	17.0682	16.1072	0.0268	3.9993

5.2.3 Three parabolic chirps and Gaussian atom

A simple signal composed of three parabolic chirps and Gaussian atom is being considered. Signal is analyzed by various t-f distributions as shown in Fig 5.3. GT gives CT free, but blurred representation. WD suffers from both inner interference

and outer interference. Inner interference is suppressed to large extent in PWD, but it still suffers from outer interference and we can see 3 extra chirp signals. PAGE distribution is hardly readable. ZAM suppresses both inner and outer interference to large extent but auto-terms also get blurred. GWT suppresses CT to large extent. Lower most quadratic chirp can be seen clearly in GWT. However, upper two chirps and Gaussian atom still suffers from interference of CT. Proposed approach gives clearly displays all four chirps and Gaussian atom. This fact can be verified by the quantitative analysis given in table 5.3. Entropy measures are minimum for the proposed approach. However, the proposed scheme has second largest value for ratio of norms measure.

TABLE 5.3: Three quadratic chirps and Gaussian atom

T-F Representation	Shannon	Renyi	Ratio of Norms	Ljubisa
PAGE	16.1537	14.97	0.0766	0.7406
Pseudo-WD	16.0619	14.77	0.0736	1.8951
ZAM	16.6215	14.41	0.2244	1.2143
GT	16.0455	15.20	0.0459	2.0101
GWT	14.7545	13.43	0.1907	0.3010
The Proposed Approach	14.3687	13.26	0.1994	0.1884
WD	17.0888	15.95	0.0322	3.7449

5.2.4 Five Gaussian atoms

In this scenario, a signal composed of five Gaussian atoms is being considered. Its t-f representations are shown in Fig 5.4. Its GT image is blurred but clearly displays all the five components. WD due to its CT problem wrongly displays thirteen Gaussian atoms. PWD reduces CT to large extent, but its still shows two extra Gaussian atoms. ZAM removes CT to great extent but quality of auto-terms is compromised. PAGE distribution also wrongly displays nine Gaussian atoms. GWT gives good performance in this scenario and most of the CT have been eliminated and quality of auto-terms is preserved. However, regions where auto-terms overlap CT, that is Gaussian atom appearing in center, still suffers from CT. Proposed approach presented clearly resolve all the Gaussian atoms and does not

TABLE 5.4: 5 Gaussian Atoms

T-F Representation	Shannon	Renyi	Ratio of Norms	Ljubisa
PAGE	13.2785	11.5663	0.0011	0.1373
Pseudo WD	13.8332	12.5356	0.0004	0.6561
ZAM	14.9510	13.0076	0.0003	3.3702
GT	13.8886	13.0272	0.0002	1.2088
GWT	12.2894	11.4489	0.0006	0.1324
The Proposed Approach	12.26	11.4014	0.0006	0.1267
WD	14.1066	12.8008	0.0004	0.5293

suffer from CT interference problem. Quantitative analysis given in table 5.4 also shows that entropy measures are minimum for the proposed approach. However, the proposed scheme has second largest value for ratio of norms measure.

5.2.5 Bat Signal

In this scenario, a real life bat signal is considered. This signal is widely used for evaluating t-f distribution. This signal is different from all synthetic signals that we have considered so far. There is a significant variation in the relative amplitudes of its components. Its t-f representations are shown in Fig 5.5. GT image is blurred, but clearly displays all the components. WD suffers from CT problem. PWD reduces CT to an extent, but still it is difficult to separate signal from CT visually. ZAM removes CT but auto-terms also get blurred. In GWT upper two chirps are not visible at all. Main reason for elimination of upper two chirps is that these chirps are of lesser magnitude. Therefore, multiplication operation has further lowered their strength. Proposed approach clearly displays all signal components without CT. All entropy based measures shown in table 5.5 gives minimum entropy value for the proposed scheme. However, ratio of norms is maximum for GWT.

TABLE 5.5: Bat Signal

T-F Representation	Shannon	Renyi	Ratio of Norms	Ljubisa
PAGE	15.17	14.19	0.0001	3.7244
Pseudo WD	14.87	13.17	0.0003	2.4427
ZAM	15.02	13.54	0.0002	3.5857
GT	14.26	13.16	0.0002	1.84
GWT	12.32	10.74	0.0015	0.0927
The Proposed Approach	10.60	10.77	0.0012	0.0593
WD	15.22	13.22	0.0004	2.127

5.3 Comparison with schemes of Similar Performance

In section 5.3, we have demonstrated the superiority of proposed scheme w.r.t kernel based schemes and GWT. Moreover, the proposed scheme has an added advantage of being fully automatic. Scheme proposed by Qazi et al. (2007) and S-method are also fully automatic CT suppression schemes that can achieve the auto-term quality equal to that of WD with no CT. In the following sub-sections we will compare the proposed scheme with these schemes on the basis of compuational cost and readibility criteria.

Comparison with scheme based on fractional Fourier Transform and signal synthesis The computational cost of proposed scheme is less than the computational cost of scheme proposed Qazi et al. (2007) for CT suppressed WD. For the signal given in 4.25, their scheme would require 3-iterations and at least 20 computations of WD in single iteration, thus making total of 60 WD computations. Whereas, the proposed technique proposed obtains the desired t-f representation by computing 3 WDs and 4 GTs. There are three signal components so 3 WDs and 3 GTs are computed for computing the desired t-f representation while one additional computation of GT is done initially for the identification of signal components thus making the total number of GT computations equal to 4. Moreover, the proposed scheme is non recursive and inherently parallel. Therefore, once

the GT image is segmented, subsequent steps can be executed in parallel on different hardware platforms and the computational cost can be further reduced to $O(N_s^2 log N_s)$

Comparison with S-method and its variants Stankovic (1994) proposed a computationally efficient S-method for computing suppressed interference WD. However, the proposed scheme has an added advantage of separating the signal components; therefore the readability of much weaker component can be made as good as that of the strongest component by uniformly scaling the t-f distributions before adding them up. This fact can be verified by considering a bat signal. All t-f representations that we have considered so far do not clearly displays two weak chirps. However, by uniformly scaling t-f distributions of separated signal components, a t-f distribution can be obtained in which all components are clearly displayed as shown in Fig 5.6.

5.4 Conclusion

In this chapter, we have demonstrated the superiority of the proposed scheme with respect to kernel based schemes both on the basis visual interpretation and quantitative evaluation. Moreover, efficacy of the proposed scheme with respect to schemes of similar performance is demonstrated on the basis of computational cost and its ability to give better readable results for much weaker signal components.

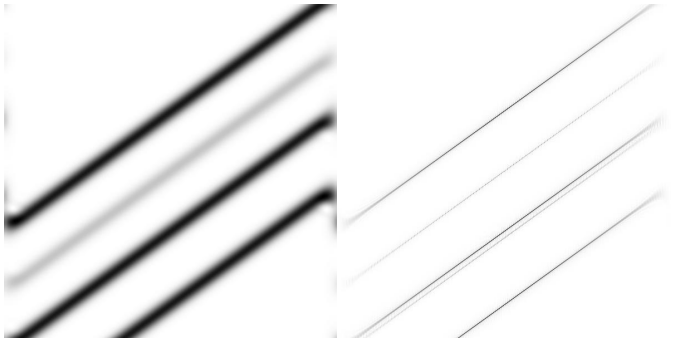

(a) (b)

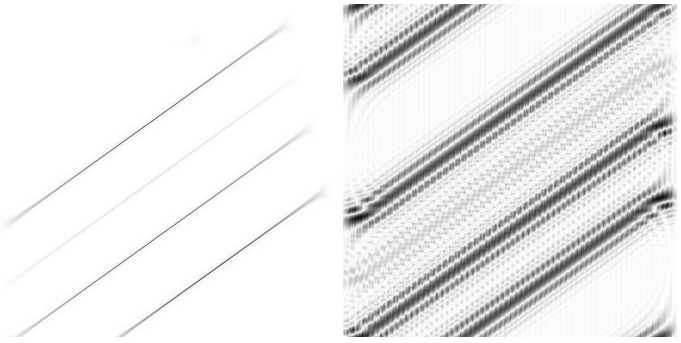

(c) (d)

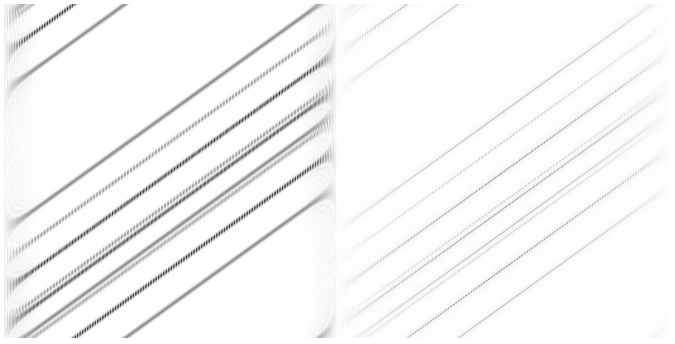

(e) (f)

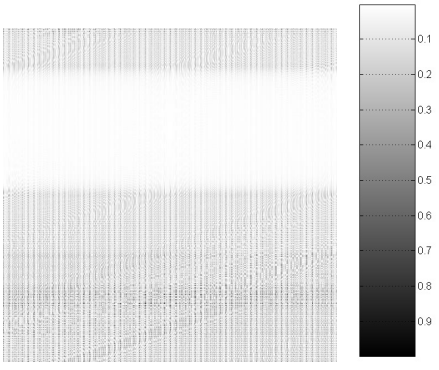

(g)

FIGURE 5.1: (a) GT (b) GWT (c) The Proposed Approach (d) ZAM (e)PWD (f)WD (g)Page

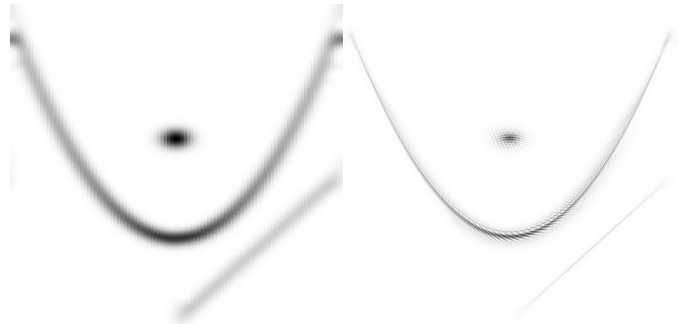

(a) (b)

(c) (d)

(e) (f)

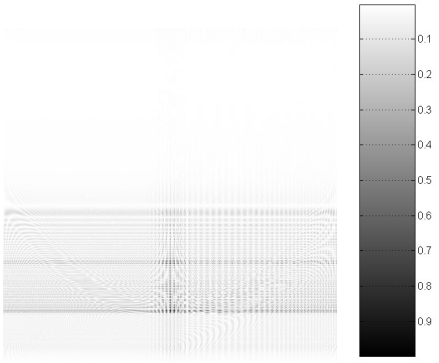

(g)

FIGURE 5.2: (a) GT (b) GWT (c) The Proposed Approach (d) ZAM (e)PWD (f)WD (g)Page

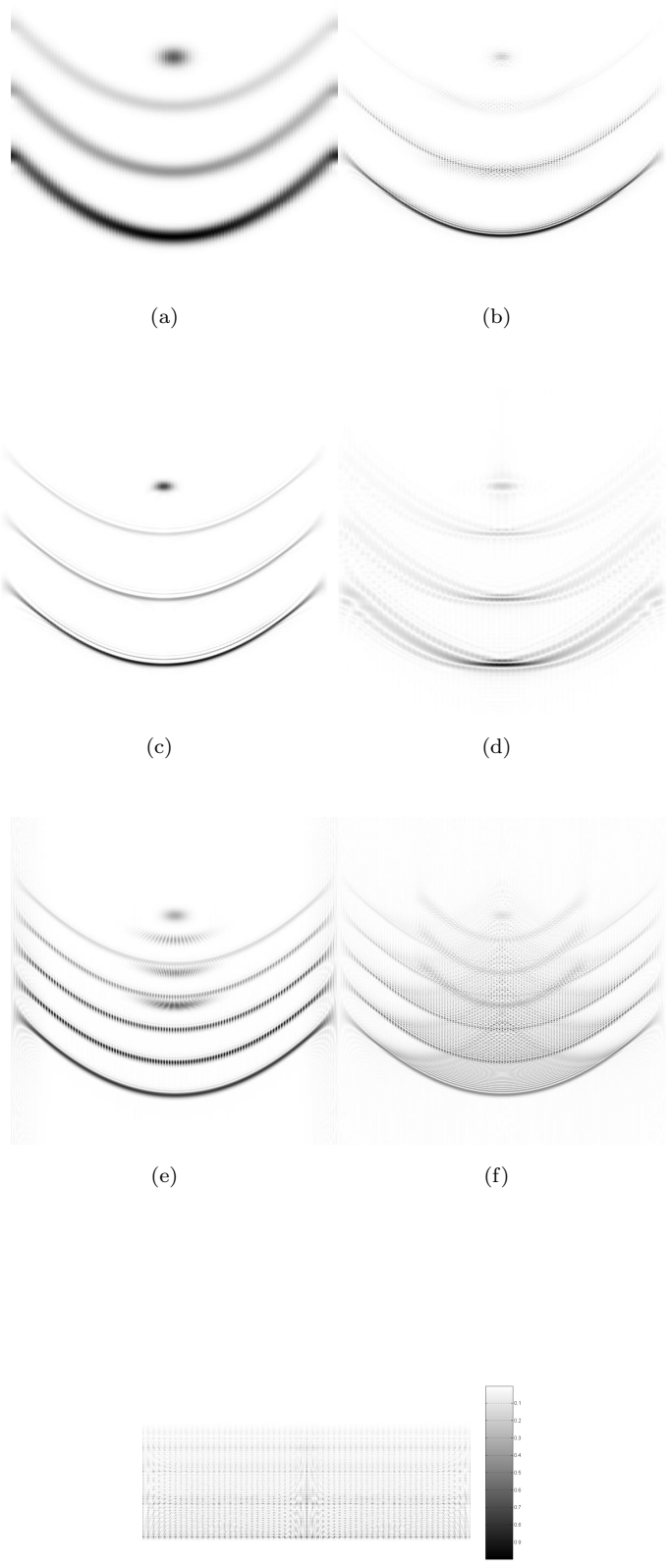

(a) (b) (c) (d) (e) (f) (g)

FIGURE 5.3: (a) GT (b) GWT (c) The Proposed Approach (d) ZAM (e)PWD (f)WD (g)Page

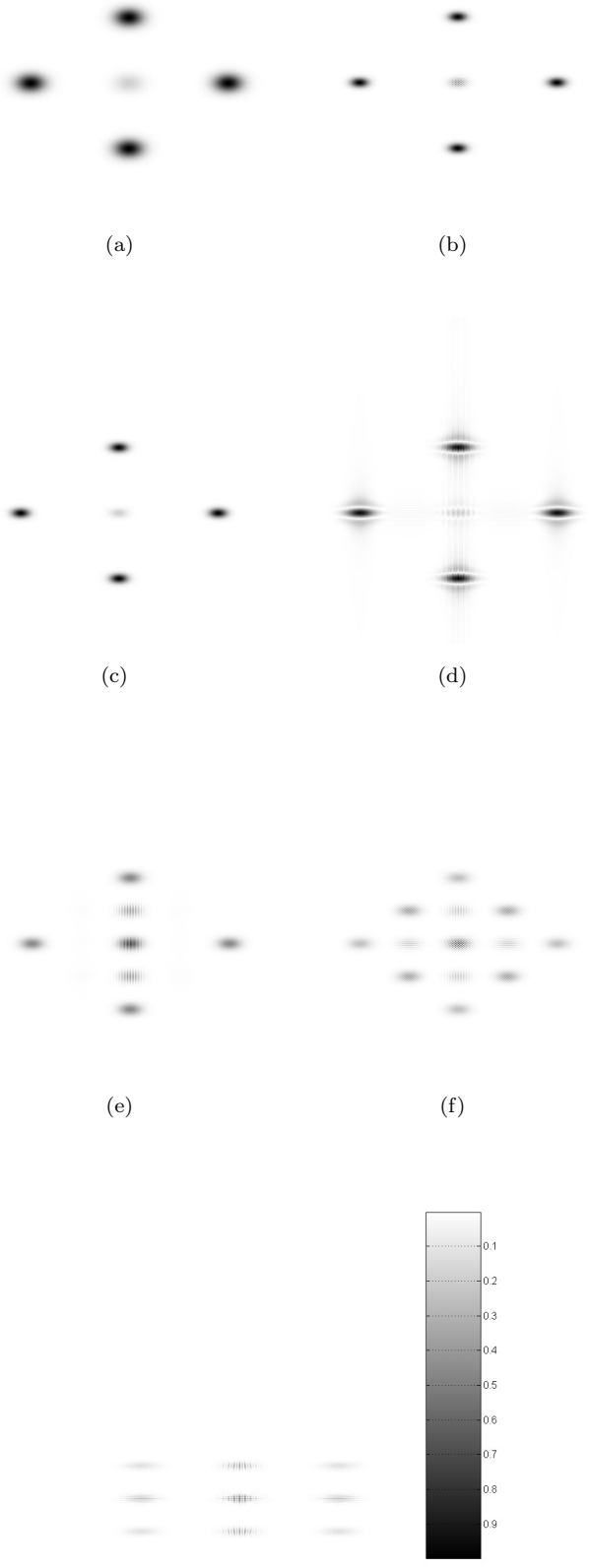

FIGURE 5.4: (a) GT (b) GWT Transform (c) The Proposed Approach (d) ZAM (e)PWD (f)WD (g)Page

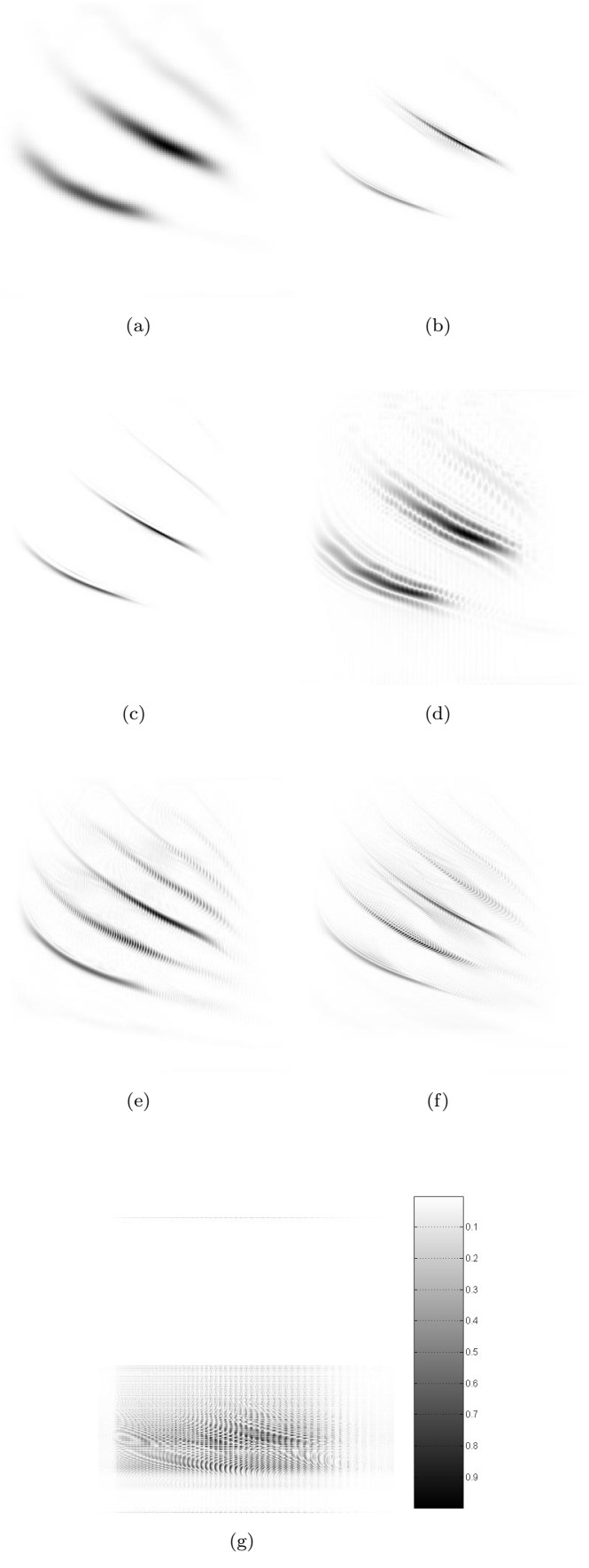

(a) (b) (c) (d) (e) (f) (g)

FIGURE 5.5: (a) GT (b) GWT (c) The Proposed Approach (d) ZAM (e)PWD (f)WD (g)Page

FIGURE 5.6: T-F representation obtained by uniformly scaling signal components

Chapter 6

INSTANTANEOUS FREQUENCY ESTIMATION

This Chapter presents IF estimation technique proposed by Khan et al. (2010) for multi-component signals corrupted by noise. The proposed technique firstly computes GT of multi-component signal to obtain location of signal components in t-f plane. The GT image is then de-noised using 2nd order partial differential equations (PDE). The de-noised image is then converted into a binary image by applying an adaptive threshold. The binary t-f image is then segmented and fractional filters are applied to separate the signal components. Finally, a well known IF estimation scheme based on WD with data dependent adaptive window length is employed to compute IF of the separated signal components. The block diagram of proposed approach is given in Fig 6.1.

Rest of the Chapter is organized as follows. Review of IF estimation schemes is given in section 6.1. Section 6.2 formulates the problem. Signal separation technique is described in section 6.3. Section 6.4 gives the algorithm of IF estimation based on WD with adaptive window length. Results are given in section 6.5.

6.1 Review of IF Estimation Schemes

IF of a non-stationary signal is an important parameter and it has applications in radar, biomedical signal analysis and motion parameter estimation as discussed by Boashash (1992); Wang and Amin (1998); Boarshash and Mesbah (2001); Djurovic and Stankovic (2003). IF is usually estimated by detecting the peak magnitude in t-f distribution at an instant. WD is widely used distribution for IF estimation. It gives an ideal IF estimate for linearly frequency modulated signals. However, it gives biased IF estimate for non-linearly frequency modulated signals. The bias can be overcome by computing windowed WD. However, windowing on one

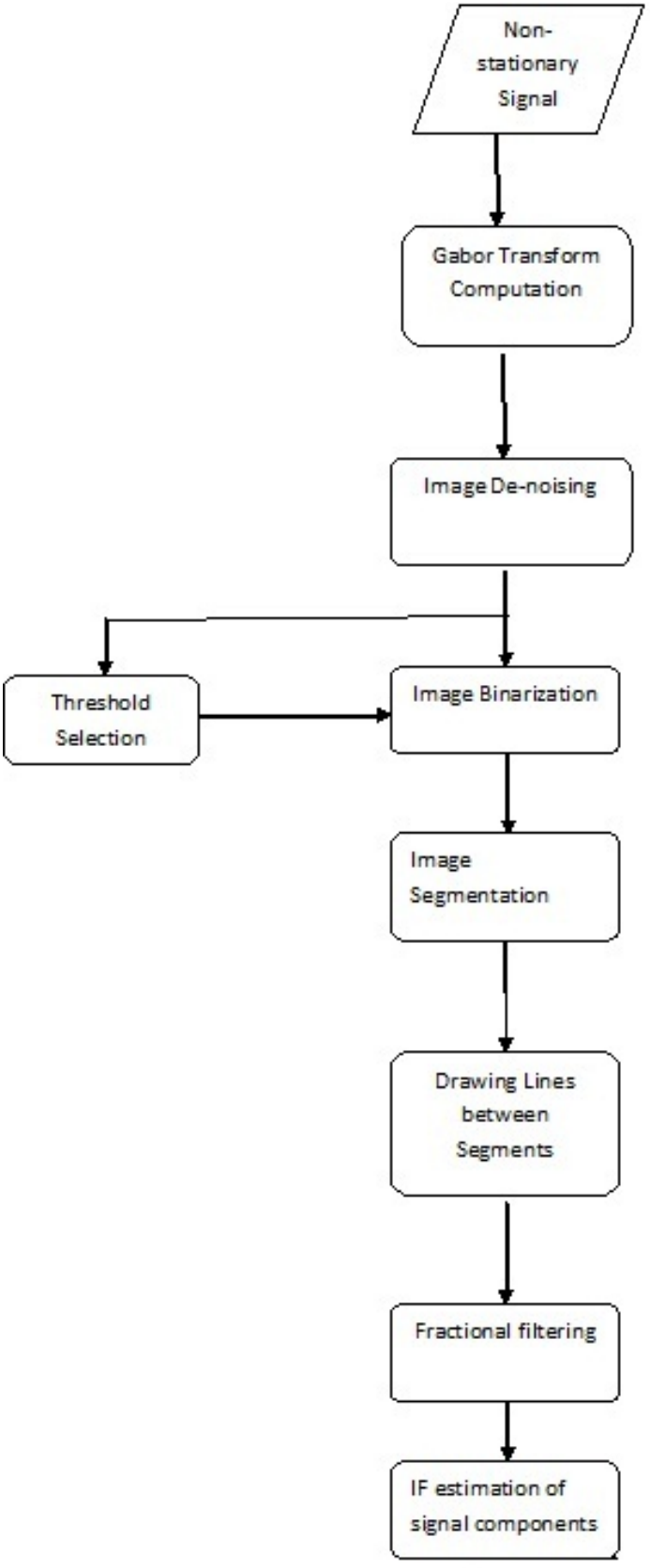

FIGURE 6.1: Block Diagram representation of Proposed technique

hand reduces the bias while on another hand it increases the variance of IF estimate. Thus there is trade off between variance and bias. Katkovnik and Stankovic (1998) proposed a technique for selection of optimal window for computation of IF. Scheme is based on Intersection of the confidence interval (ICI) rule. WD with adaptive window length is a useful technique, but it can only be applied to mono-component signals.

Hussain and Boashash (2002) extended WD with adaptive window length for multi-component signals. This scheme requires tracking of maxima of each signal component while ignoring the local maxima caused by cross terms. However this technique requires a prior t-f analysis to locate signal components and manual selection of thresholds. Therefore this technique is not fully automatic. Rankine et al. (2007) presented image processing based fully automatic technique for IF estimation of multi-component signals. A t-f representation with reduced interference is obtained by computing modified B-distribution and the IF is estimated by peak detection. It is assumed that the signal components have non overlapping t-f representation, therefore a connectivity criterion is applied after peak detection to obtain IF estimates of the signal components. One of the limitations of this scheme is that the modified B-distribution fails to give good CT suppression if the signal components have significant frequency modulation. In another study, Baihe Wang (2007) applied Viterbi algorithm for IF estimation of multi-component signal corrupted by high noise environment. However, that scheme can only be applied for IF estimation of linearly frequency modulated signals.

6.2 Problem Formulation

Consider a multi-component signal, $s(t)$, composed of a sum of mono-component signals corrupted by additive white Gaussian noise. Mathematically,

$$s(t) = \sum_{i=1}^{N} s_i(t) + n(t), \qquad \textit{Eq (6.1)}$$

where

$$s_i(t) = A_i e^{j\phi_i(t)}. \qquad Eq\ (6.2)$$

A_i is the amplitude and $\phi_i(t)$ is the instantaneous phase of signal component $s_i(t)$. N is total number of signal components. IF of each component is defined as

$$f_i(t) = \frac{1}{2\pi}\frac{d\phi_i(t)}{dt}. \qquad Eq\ (6.3)$$

One way to compute IF is by detecting the peak in t-f distribution of the signal components. Mathematically,

$$f_i(t) = \underset{\omega}{argmax}\, TF_i(t,\omega). \qquad Eq\ (6.4)$$

$TF_i(t,\omega)$ is a t-f representation of signal component $s_i(t)$. In order to compute t-f representation of individual signal component, the signal components must be extracted from a composite signal. The signal components can be separated by hybrid image processing and fractional Fourier based technique presented in the next section.

6.3 Modified signal separation scheme based on Fractional Filtering

This section presents the modified version of fractional Fourier transform based signal separation scheme presented in chapter 4. In the signal separation scheme, we only considered noise free signals, therefore for signals corrupted by additive white Gaussian noise, a anisotropic diffusion based image de-noising step has been added. In sub-section 6.3.1, summary of the modified signal separation scheme is presented. While in sub-section 6.3.2, t-f denoising scheme is discussed in detail.

6.3.1 Signal Separation Scheme

Major steps of the signal separation scheme are

1. Gabor Transform computation: Approximate locations of the signal components is obtained by computing GT. GT is chosen as it gives cross-term free t-f representation.

2. Time frequency image de-noising: GT image is denoised using partial differential equations.

3. Image thresholding: The de-noised grey scale t-f image is converted into a binary image by applying a threshold. All pixels having magnitude greater than a chosen threshold are assigned one while zero is assigned to all other pixels.

4. Image Segmentation: Binary image separates regions separates foreground from background. It is assumed that signal components have non-overlapping t-f signature. Therefore, foreground of binary image is decomposed into N number of segments.

5. Drawing lines between segments: Segments are separated by drawing lines between them as discussed in chapter 4.

6. Fractional Filtering: Signal components are separated by applying fractional filters.

6.3.2 Time Frequency image De-noising

GT image is composed of foreground where signal components are present and background where no signal component is present. These background and foreground regions can be identified by applying a suitable threshold. However, noise may cause foreground region to appear as background and background may appear as foreground. Therefore de-noising algorithm must be applied before the t-f image is converted into binary image. Mean filtering, median filtering and Gaussian filtering are standard methods of removing noise from image at the cost of blurring of edges. Unfortunately, blurring of edges may cause two closely placed

signal components to merge in t-f plane. Anisotropic diffusion proposed by Perona and Malik (1990), where image grey level changes are modeled as a second order partial differential equation derived from the heat equation, has emerged as power full tool of image enhancement. This model is based on intuition that smoothing must be performed inside object boundaries not across it. This has a direct analogy with heat equation that flow of heat across the boundaries of different object is constrained by diffusion co-efficient. Mathematically anisotropic diffusion equation is given by,

$$\frac{\partial GT_\tau(t,\omega)}{\partial \tau} = c(t,\omega,\tau)\Delta G_\tau(t,\omega) + \nabla c(t,\omega,\tau)\nabla G_\tau(t,\omega). \qquad Eq\ (6.5)$$

∇ and Δ are gradient and laplacian operations respectively. $c(t,\omega,\tau)$ parameter controls smoothing inside and outside image boundaries. Ideally it should be zero on boundary. Information regarding image boundaries can be obtained from image gradient. Let g be a decreasing function, then

$$c(t,\omega,\tau) = g(|\nabla GT_\tau(t,\omega)|). \qquad Eq\ (6.6)$$

6.4 Adaptive Instantaneous Frequency estimation

In this section, we present the summary of IF estimation technique based on WD with adaptive window length proposed by Rankine et al. (2007). Following steps are performed for each of the separated signal components.

1. Separated signal components $s_i(t)$ obtained as a result of fractional filtering suffer from the filtered noise. Amplitude A_i and noise variance σ_i of signal component can be estimated using a method based on higher order moments proposed by Sekhar and Sreenivas (2006)

$$A_i = \sqrt{|2E[s_i^2(t)]^2 - E[s_i^4(t)]|}, \qquad Eq\ (6.7)$$

$$\sigma_i = |E[s_i^2(t)] - \sqrt{|2E[s_i^2(t)]^2 - E[s_i^4(t)]|}|. \qquad Eq\ (6.8)$$

2. Signal components are analyzed using multiple PWDs. Mathematically,

$$PWD_{i,h_k}(t,\omega) = \int h_k(\tau) s_i(t-\tau/2) s_i^*(t+\tau/2) e^{-j\omega\tau} d\tau. \qquad Eq\ (6.9)$$

$h_k(\tau)$ is hamming window selected from set of increasing window lengths $H = h_k = h_0 2^k, k = 0, 1, 2, ...J$

3. In order to suppress the inner-interference PWDs of separated signal component are multiplied with their GTs. Mathematically,

$$BPWD_{i,h_k}(t,\omega) = PWD_{i,h_k}(t,\omega) GT_i(t,\omega). \qquad Eq\ (6.10)$$

4. IF is estimated from all the PWDs by peak detection. Mathematically,

$$\widehat{f}_{i,h_k}(t) = \underset{\omega}{argmax}\, BPWD_{i,h_k}(t,\omega). \qquad Eq\ (6.11)$$

5. Check the IF estimates obtained from window length h_k and h_{k-1} for following inequality

$$|\widehat{f}_{i,h_k}(t) - \widehat{f}_{i,h_{k-1}}(t)| \leq (\kappa+1)(\sigma_i(h_k) + \sigma_i(h_{k-1})) \qquad Eq\ (6.12)$$

$\sigma_i(h_k)$ is the variance of window h_k for signal component $s_i(t)$ that can be computed by the method described in Katkovnik and Stankovic (1998). If the IF estimate do not fulfill above mentioned inequality, then IF estimate obtained from h_{i-1} is chosen to be desired IF estimate. Otherwise, k is incremented and step 5 is repeated till we reach the largest window.

6.5 Results

In order to evaluate performance of our algorithm we consider two different multi-component signals. The first one is composed of two quadratic chirps and the second one is composed of two triangular chirps.

6.5.1 Two Quadratic Chirps

Signal composed of two quadratic chirps is being considered. Mathematically,

$$s(t) = e^{j(18\pi t^3 + 104\pi t)} + e^{j(18\pi t^3 + 8\pi t)} \qquad Eq\ (6.13)$$

The sampling frequency is chosen to be 200Hz and the signal duration is taken to be from 1.5s to 1.5s. The signal is corrupted by additive white Gaussian noise of 5db. Original and de-noised Gabor Transform images are shown in Fig 6.2(a) and Fig 6.2(b) respectively. Two binary images, obtained by thresholding the original image and the de-noised image, are shown in Fig 6.2(c) and Fig 6.2(d). It is clear that the binary image obtained from the de-noised image better separates the signal components from noise. Finally IFs of separated signals are plotted against their original IF as shown in Fig 6.2(e).

6.5.2 Two Triangular Chirps

Multi-component signal composed of two triangular chirps with different amplitudes is being considered. Mathematically,

$$s(t) = e^{j(|30\pi t^2| + 76\pi t)} + 0.5e^{j(|30\pi t^2| + 4\pi t)} \qquad Eq\ (6.14)$$

The sampling frequency is chosen to be 200Hz and the signal duration is taken to be from -1.5s to 1.5s. The signal is corrupted by additive white Gaussian noise of 6db. The original and the de-noised Gabor Transform images are shown in Fig 6.3(a) and Fig 6.3(b) respectively. Two binary images, obtained by thresholding the original and de-noised images, shown in Fig 6.3(c) and Fig 6.3(d) respectively,

clearly demonstrate that the de-noised image better separates the signal components from noise. Finally IFs of the separated signals are plotted against their original IFs as shown in Fig 6.3(e).

(a)

(b)

(c)

(d)

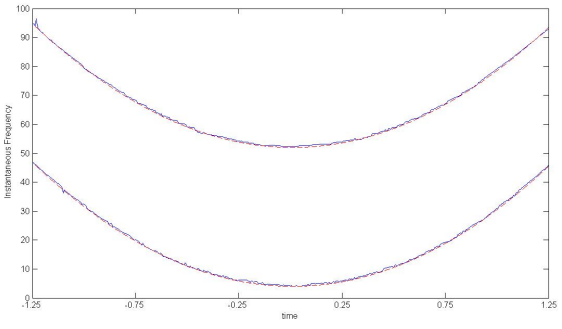

(e)

FIGURE 6.2: a) GT image b) De-noised Image, c) Binary Image d) De-noised Binary Image e) IF plot vs IF estimated

(a) (b)

(c) (d)

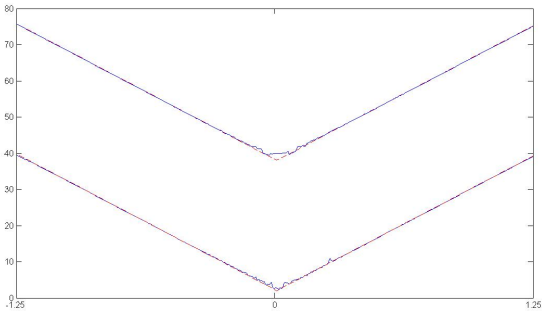

(e)

FIGURE 6.3: a) GT image b) De-noised Image, c) GT image binary d) De-noised image binary e) IF plot vs IF estimated

Chapter 7

CONCLUSION AND FUTURE WORK

7.1 Conclusion

The thesis presents following two major contributions

1. CT Suppression in WD: We have presented a t-f representation based on image processing and fractional filtering, that has significantly reduced CT and has auto-term quality equal to that of WD. The proposed scheme is computationally efficient and fully automatic. Performance of the proposed technique is evaluated on the basis of energy concentration, readability and CT suppression criterion. Energy concentration is evaluated on the basis of entropy based measures while readability is judged on the basis of visual inspection. It has been demonstrated that the proposed scheme out performs GWT and kernel based t-f representations both on the basis of visual inspection and quantitative measures. Computational cost of the proposed scheme is more than kernel based schemes. However, it is less than the scheme of similar performance Qazi et al. (2007). It has also been demonstrated that proposed scheme can give clear representation of much weaker signal components.

2. IF estimation: An effective IF estimation scheme based on signal separation and WD with adaptive window length has been presented. Signal separation technique employed for CT elimination is slightly modified with the addition of PDE based image de-noising step. This scheme is fully automatic and does not make any assumption about IF laws of signal components. However, the IF estimation scheme suffers from same limitations as that of the CT suppression scheme. Thus, any improvement in the signal separation scheme would automatically improve the IF estimation scheme.

7.2 Future Work

There are following limitations of proposed scheme and they can be overcome in future work.

1. Resolution Limitation: The signal separation scheme computes GT to obtain coarse t-f representation which is subsequently processed to obtain a t-f representation that gives high energy concentration. Reason for choosing GT for obtaining coarse representation is that it is a linear transformation and does not suffer from CT. However, it suffers from resolution limitation in dealing with closely placed signal components. This problem can be partially overcome either by employing other linear transforms that can give high resolution like Wavelet transform, Spectrogram using windows in fractional domain proposed by Capus and Brown (2003) or by using de-blurring techniques such as, de-blurring of spectrogram using neural networks proposed by Shafi et al. (2007) or de-blurring using image de-convolution technique proposed by kai Lu and Zhang (2009). However, employing de-blurring techniques will increase the computational cost.

2. Separable auto-terms: The proposed scheme can only be applied to signals with separable auto-terms and cannot cater for signals with overlapping auto-terms like crossing chirps. This constraint can be overcome by more intelligent image segmentation techniques which should also incorporate the continuity of t-f signature of signals.

3. Adaptive Thresholding: The proposed scheme applies a global threshold to form a binary image. Better results can be obtained by applying a region dependent adaptive threshold.

4. Signal decomposition: The proposed scheme decomposes signal whose auto-terms are not linearly separable in t-f plane. These decomposed signals are independently processed. Discontinuities are introduced when such signal

components are put together. This problem can be solved for certain class of signals by repeated filtering in consecutive fractional Fourier domains proposed by Erden et al. (1999).

5. Improved IF estimation of mono-component signal: The proposed scheme computes IF of the separated component using ICI rule. Recently modified ICI rule has been presented by Lerga and Sucic (2009) that gives more accurate IF estimate for mono-component signal. Thus, modified ICI rule can be used to compute IF from a separated mono-component signal.

6. Image De-noising : We have employed PDE based image de-noising scheme. One of the limitation of PDE based scheme is its iterative nature and thus a computational cost. There has been lot of research going on image de-noising schemes. Better and more computationally efficient schemes may be applied to improve the performance of existing schemes.

Proposed t-f representation can be applied for following engineering problems.

1. Motion Estimation: Djurovic and Stankovic (2003) used t-f distributions for computing velocity and position of slow moving objects in sequence of images. Synthetic images containing information about the motion parameters is obtained by projecting video on the coordinate axes. These synthetic images are mapped to the frequency modulated signals by using constant u-propagation. Thus the problem of velocity estimation is reduced into the problem of IF estimation. In case of single moving object frequency modulated signal would be a mono-component signal while in case of multiple moving objects frequency modulated signal would be composed of multiple components. In case of single moving object WD gives best estimates of motion parameters. However, in case of multiple moving objects WD cannot be applied because of CT problem. The proposed t-f representation removes CT of WD to great extent, therefore the proposed scheme can be used for computing accurate estimates of motion parameters.

2. Channel estimation Problem: Shen and Papandreou-Suppappola (2006) proposed a channel estimation scheme based upon t-f representation. Parabolic chirp signal is transmitted as a training signal through a time varying channel. Parabolic chirp signal is de-chirped at the receiver to obtain a combination of linear chirps. Modified matching pursuit algorithm is applied to obtain the parameters of linear chirps from the received signal. These parameters are used to obtain the parameters of channel. T-f representation proposed in this study is computationally efficient as compared to matching pursuit algorithm. Therefore, it can be used instead of matching pursuit algorithm to obtain the parameters of channel in much more computationally efficient manner.

3. New Born Seizure detection: Dysfunction in the central nervous system of the neonate can be identified through seizures which can be detected from EEG signal. Newborn seizure is a multi-component signal. IF of signal components is an important feature and is used for diagnostic purpose. Recently Rankine et al. (2007) proposed an IF estimation scheme for newborn seizure detection. A direction of future work could be to compare the performance of the IF estimation scheme proposed in this thesis with the scheme presented by Rankine et al. (2007) for new born seizure detection.

REFERENCES

Acharya, T., Ray, A. K., 2005. Image Processing - Principles and Applications. Wiley-Interscience.

Arce, G., Hasan, S., Aug 2000. Elimination of interference terms of the discrete Wigner distribution using nonlinear filtering. IEEE Transactions on Signal Processing 48 (8), 2321 –2331.

Arikan, O., Kemal Ozdemir, A., 2000. An efficient algorithm to extract components of a composite signal. In: Acoustics, Speech, and Signal Processing, 2000. ICASSP '00. Proceedings. 2000 IEEE International Conference on. Vol. 2. pp. II697 –II700 vol.2.

Auger, F., Flandrin, P., May 1995. Improving the readability of time-frequency and time-scale representations by the reassignment method. IEEE Transactions on Signal Processing 43, 1068 1089.

Bai-he Wang, J.-g. H., 2007. Instantaneous frequency estimation of multi-component chirp signals in noisy environments. Journal of Marine Science and Application 6 (4), 13–17.

Baraniuk, R., Jones, D., Apr 1993. A signal-dependent time-frequency representation: optimal kernel design. IEEE Transactions on Signal Processing 41 (4), 1589 –1602.

Bastiaans, M., Alieva, T., Stankovic, L., Nov 2002. On rotated time-frequency kernels. IEEE Signal Processing Letters 9 (11), 378 – 381.

Boarshash, B., Mesbah, M., Sep/Oct 2001. A time-frequency approach for newborn seizure detection. Engineering in Medicine and Biology Magazine, IEEE 20 (5), 54 –64.

Boashash, B., 1992. Estimating and interpreting the instantaneous frequency of a signal. i. fundamentals. Proceedings of the IEEE 80 (4), 520–538.

Boashash, B. (Ed.), 2003. Time-Frequency Signal Analysis and Processing: A Comprehensive Reference. Elsevier Science, Oxford.

Boashash, B., O'Shea, P., Jan 1994. Polynomial Wigner-ville distributions and their relationship to time-varying higher order spectra. IEEE Transactions on Signal Processing 42 (1), 216 –220.

Boudreaux-Bartels, G., Parks, T., June 1986. Time-varying filtering and signal estimation using Wigner distribution synthesis techniques. IEEE Transactions on Acoustics, Speech and Signal Processing 34 (3), 442 – 451.

Capus, C., Brown, K., 2003. Short-time fractional Fourier methods for the time-frequency representation of chirp signals. The Journal of the Acoustical Society of America 113 (6), 3253–3263.
URL `http://link.aip.org/link/?JAS/113/3253/1`

Chapelle, O., 2007. Training a support vector machine in the primal. Neural Comput. 19 (5), 1155–1178.

Cohen, L., Jul 1989. Time-frequency distributions-a review. Proceedings of the IEEE 77 (7), 941 –981.

Djurovic, I., Stankovic, S., May 2003. Estimation of time-varying velocities of moving objects by time-frequency representations. IEEE Transactions on Image Processing 12 (5), 550 – 562.

Erden, M., Kutay, M., Ozaktas, H., May 1999. Repeated filtering in consecutive fractional Fourier domains and its application to signal restoration. IEEE Transactions on Signal Processing 47 (5), 1458 –1462.

Fulop, S. A., Fitz, K., 2006. A spectrogram for the twenty-first century. Acoustics Today 2 (3), 26–33.

Hlawatsch, F., Boudreaux-Bartels, G., Apr 1992. Linear and quadratic time-frequency signal representations. IEEE Signal Processing Magazine 9 (2), 21 –67.

Hlawatsch, F., Manickam, T. G., Urbanke, R. L., Jones, W., 1995. Smoothed pseudo-Wigner distribution, Choi-williams distribution, and Cone-kernel representation: Ambiguity-domain analysis and experimental comparison. Signal Processing 43 (2), 149 – 168.
URL http://www.sciencedirect.com/science/article/B6V18-3YS8YJN-F/2/9ff9455c710eb77b58ce33fcbe700935

Hsu, C. W., Chang, C. C., Lin, C. J., 2003. A practical guide to support vector classification. Tech. rep., Taipei.
URL http://www.csie.ntu.edu.tw/~{}cjlin/papers/guide/guide.pdf

Hussain, Z., Boashash, B., Aug 2002. Adaptive instantaneous frequency estimation of multicomponent fm signals using quadratic time-frequency distributions. IEEE Transactions on Signal Processing 50 (8), 1866 –1876.

Jones, D., Baraniuk, R., Oct 1995. An adaptive optimal-kernel time-frequency representation. IEEE Transactions on Signal Processing 43 (10), 2361 –2371.

Jones, D., Parks, T., Feb 1992. A resolution comparison of several time-frequency representations. IEEE Transactions on Signal Processing 40 (2), 413 –420.

kai Lu, W., Zhang, Q., July 2009. Deconvolutive short-time Fourier transform spectrogram. IEEE Signal Processing Letters 16 (7), 576 –579.

Katkovnik, V., Stankovic, L., Sep 1998. Instantaneous frequency estimation using the Wigner distribution with varying and data-driven window length. IEEE Transactions on Signal Processing 46 (9), 2315 –2325.

Khan, N., Jaffri, M., Shah, S., 3-5 2009. Modified Gabor Wigner transform for crisp time frequency representation. In: International Conference on Signal Acquisition and Processing, 2009. ICSAP 2009. pp. 119 –122.

Khan, N., Taj, I., Jaffri, M., 9-10 2010. Instantaneous frequency estimation using fractional Fourier transform and Wigner distribution. In: International Conference on Signal Acquisition and Processing, 2010. ICSAP '10. pp. 319 –321.

Khan, N. A., Taj, I. A., Jaffri, M. N., Ijaz, S., 2011. Cross-term elimination in Wigner distribution based on 2D signal processing techniques. Signal Processing 91 (3), 590 – 599, advances in Fractional Signals and Systems.
URL http://www.sciencedirect.com/science/article/B6V18-508PPN4-1/2/e25c7de2ab19e6baa9d4224e7190809c

Lang, W. Christopher; Forinash, K., Feb. 1999. Time-frequency analysis with the continuous wavelet transform. American Journal of Physics 67 (10), 934–935.

Lerga, J., Sucic, V., Nov. 2009. Nonlinear IF estimation based on the pseudo WVD adapted using the improved sliding pairwise ici rule. IEEE Signal Processing Letters 16 (11), 953 – 956.

Mallat, S., Zhang, Z., Dec 1993. Matching pursuits with time-frequency dictionaries. IEEE Transactions on Signal Processing 41 (12), 3397 –3415.

Mustard, D., 1996. The fractional Fourier transform and the Wigner distribution. The ANZIAM Journal 38 (02), 209–219.
URL http://journals.cambridge.org/action/displayAbstract?fromPage=online&aid=3979672&fulltextType=RA&fileId=S0334270000000606

Namias, V., 1980. The fractional order Fourier transform and its application to quantum mechanics. IMA J Appl Math 25 (3), 241–265.
URL http://imamat.oxfordjournals.org/cgi/content/abstract/25/3/241

Pachori, R. B., Sircar, P., 2007. A new technique to reduce cross terms in the Wigner distribution. Digit. Signal Process. 17 (2), 466–474.

Pei, S.-C., Ding, J.-J., Oct. 2007. Relations between Gabor transforms and fractional Fourier transforms and their applications for signal processing. IEEE Transactions on Signal Processing 55 (10), 4839 –4850.

Perona, P., Malik, J., Jul 1990. Scale-space and edge detection using anisotropic diffusion. IEEE Transactions on Pattern Analysis and Machine Intelligence 12 (7), 629 –639.

Qazi, S., Georgakis, A., Stergioulas, L., Shikh-Bahaei, M., June 2007. Interference suppression in the Wigner distribution using fractional Fourier transformation and signal synthesis. IEEE Transactions on Signal Processing 55 (6), 3150 –3154.

Rankine, L., Mesbah, M., Boashash, B., 2007. IF estimation for multicomponent signals using image processing techniques in the time-frequency domain. Signal Process. 87 (6), 1234–1250.

Sang, T.-H., Williams, W., 9-12 1995. Renyi information and signal-dependent optimal kernel design. In: Acoustics, Speech, and Signal Processing, 1995. ICASSP-95., 1995 International Conference on. Vol. 2. pp. 997 –1000 vol.2.

Sekhar, S. C., Sreenivas, T. V., 2006. Signal-to-noise ratio estimation using higher-order moments. Signal Process. 86 (4), 716–732.

Shafi, I., Ahmad, J., Shah, S., Kashif, F., June 2007. Evolutionary time-frequency distributions using bayesian regularised neural network model. IET Signal Processing 1 (2), 97 –106.

Shannon, C. E., 2001. A mathematical theory of communication. SIGMOBILE Mob. Comput. Commun. Rev. 5 (1), 3–55.

Shen, H., Papandreou-Suppappola, A., 2006. Diversity and channel estimation using time-varying signals and time-frequency techniques. IEEE Transactions on Signal Processing 54 (9), 3400 –3413.

Stankovic, L., Jan 1994. A method for time-frequency analysis. IEEE Transactions on Signal Processing 42 (1), 225 –229.

Stanković, L., 2001. A measure of some time-frequency distributions concentration. Signal Process. 81 (3), 621–631.

Stankovic, S., Stankovic, L., Jul 1997. An architecture for the realization of a system for time-frequency signal analysis. IEEE Transactions on Circuits and Systems II: Analog and Digital Signal Processing, 44 (7), 600 –604.

Wang, C., Amin, M., Jan 1998. Performance analysis of instantaneous frequency-based interference excision techniques in spread spectrum communications. IEEE Transactions on Signal Processing 46 (1), 70 –82.